Current Research in Food Science 10 (2025) 101013

Contents lists available at ScienceDirect

Current Research in Food Science

journal homepage: www.sciencedirect.com/journal/current-research-in-food-science

Computer simulation of microwave-assisted drying: Coupled influence of microwave power and pulse ratio on product and process characteristics

Jalal Dehghannya *, Mahdi Habibi-Ghods

Department of Food Science and Technology, University of Tabriz, Tabriz, 51666-16471, Iran

ARTICLE INFO

Handling Editor: Dr. Maria Corradini

Keywords:
Microwave
Pulsed drying
Mathematical modeling
Moving boundary
Convective hot air

ABSTRACT

Shrinkage consideration is pivotal in modeling heat and mass transfer during drying processes. This study investigated the interactive effects of microwave power and pulse ratio on various properties of potato slices during drying. The drying process was further modeled using moving boundary conditions to assess the influence of these variables on heat and moisture diffusion. Results demonstrated that increasing microwave power and decreasing the pulse ratio significantly reduced drying time due to intensified effective moisture diffusion coefficient (14.28%). Enhanced product quality—evidenced by minimized shrinkage (26.28%), reduced bulk density (13.22%), and improved rehydration ratio (28.96%)—alongside increased energy efficiency, was observed with higher power levels and pulse ratios. Additionally, a higher pulse ratio intensified the electric field due to shorter microwave "on" durations, promoting a more uniform wave distribution within the product. Unlike convective air drying, where moisture removal initiated from the food's edges, the combined microwave-air drying approach exhibited a distinct moisture migration pattern attributed to the volumetric heating mechanism of microwaves, which directed heat transfer from the interior to the surface of the potato slices. The model's performance, evaluated using R^2 and RMSE metrics, was deemed satisfactory. Overall, this research highlights the importance of optimizing microwave power and pulse ratio for the efficient production of high-quality potato chips.

1. Introduction

The potato, scientifically known as *Solanum tuberosum*, was introduced to Europe by the Spaniards from the Americas in the second half of the 16th century (Gomide et al., 2022). Since 2014, potatoes have been the fourth largest food crop in the world, following maize, wheat, and rice (Heshmati et al., 2023). Being carbohydrate-based, potatoes provide more energy to consumers compared to other vegetables (Devaux et al., 2021). Potatoes are inexpensive, grow easily in various climatic conditions, and contain various nutrients, including micronutrients and macronutrients (Devaux et al., 2021). There are many methods for processing potatoes, such as boiling, frying, and drying, each of which results in different organoleptic properties and affects the nutritional value of the product (Onyenwigwe et al., 2023).

Drying is one of the most important and valuable processes for preserving food materials, often associated with various quality alterations affecting customer choice (Mierzwa and Szadzińska, 2019). Drying with convective hot air is an old technique for moisture removal from food. However, its prolonged drying time and creation of a thermal gradient within the food may seriously damage the organoleptic properties of the final product, such as color (Chen et al., 2020). Microwave drying is one of the significant advancements in food industry (Chong et al., 2021).

Microwaves are located in the electromagnetic spectrum with frequencies higher than radio waves and lower than infrared waves (Rao, 2015). Microwaves are classified as non-ionizing radiation, and therefore, when food is exposed to these waves, no known non-thermal effects are produced in the food (Bakshi et al., 2023). The most critical factors that significantly affect microwave heating and its heat distribution are the dielectric properties of the food and the penetration depth (von et al., 2022). Microwave heating has wide applications in various food processing techniques, such as drying. A microwave oven is a device that generates microwave heating and can have specific applications in the food industry, such as cooking, defrosting, and drying (Erle et al., 2020).

Generally, microwave drying has three stages: heating, a constant drying rate period, and a declining drying rate period (Monteiro et al., 2020). Currently, compared to other drying methods like convective hot air, microwave drying is one of the fastest drying techniques in the food industry because microwave energy is generated directly without the

* Corresponding author.
E-mail address: J_dehghannya@tabrizu.ac.ir (J. Dehghannya).

https://doi.org/10.1016/j.crfs.2025.101013
Received 5 December 2024; Received in revised form 25 January 2025; Accepted 26 February 2025
Available online 27 February 2025

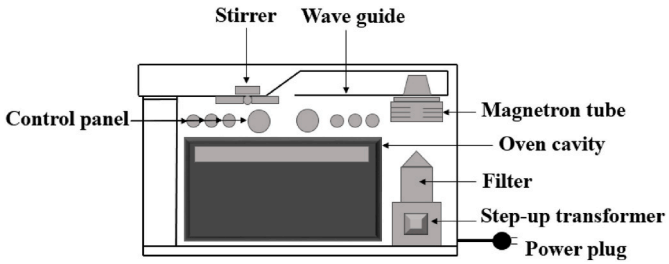

Fig. 1. A schematic of the microwave oven with its constituents.

Table 1
Different microwave pulse ratios (PR) at fixed "off" times (180 s).

Treatment	PR	Microwave "on" time	"on" and "off" cycle
1	2	180	360
2	4	60	240
3	6	36	216

need to heat the surrounding air, thus shortening the processing time. The collision between microwaves and water molecules inside the food, through the mechanisms of dipole rotation and ionic polarization, leads to volumetric heating (internal heating) of the food and increased moisture diffusion (Bakshi et al., 2023; Franco et al., 2015).

Microwaves can perform drying either intermittently (with controlled pauses at specific times) or continuously (without interruption). Alternatively, microwaves can be combined with supplementary drying techniques, such as convective hot air drying, to increase drying efficiency, reduce drying time, and enhance the final quality of the dried product (Macedo et al., 2022; Kumar and Karim, 2019). The precise selection of the pulse ratio, obtained through Eq. (1), is crucial for achieving a product with suitable quality (Dehghannya et al., 2023a).

The combined intermittent microwave-convective drying, due to microwaves unique volumetric heating capability, has attracted the attention of various researchers (Kumar and Karim, 2019; Dehghannya et al., 2023b). In this method, a significant reduction in drying time occurs due to the increased heat and mass transfer by microwaves (Kumar and Karim, 2019). Additionally, in the combined method, since hot air also assists in the drying process, there is no need to use high microwave power levels (Brahmi et al., 2023). During convective hot air drying, lower temperatures are preferred due to improved color and rehydration, although this may increase the drying time (Dehghannya et al., 2023b).

Nguyen et al. (2019) used a combination of continuous microwave and convective hot air drying to dry bitter melon (*Momordica charantia* L.) at different temperatures (20, 25, and 30 °C) and microwave power densities (1.5, 3, and 4.5 W/g). The results showed that the drying rate was faster at higher temperatures due to faster heat and mass transfer. However, during the initial drying period, the drying rate in the combined method was faster than in convective hot air drying. This result was attributed to the high initial moisture content in the sample, which led to more substantial microwave absorption and consequently increased moisture diffusion. Microwave absorption decreased in the final drying stage due to lower moisture content. The rehydration ratio intensified with higher power density. This was associated with the more significant internal stresses created during drying at higher microwave power and more structural damage to the food material.

Heshmati et al. (2023) performed simultaneous modeling of heat and mass transfer during potato drying using a combined continuous microwave and hot air. The results showed that heat distribution within the product became more uniform with increased drying time. The modeling data showed that the product lost its surface moisture after 10 min of drying. After 50 min, moisture removal slowed down due to a more minor moisture difference between the internal and external layers of the food material. The moisture content of the internal layers reached equilibrium moisture after 70 min of processing. In this study, electromagnetic wave modeling was not performed and Lambert's equation was used as a heat source. Moreover, microwave intermittency and shrinkage (moving boundary) were not incorporated in the modeling.

Based on available sources, no assessment has dealt with the joint modeling of electromagnetic waves, heat, and mass transfer incorporating shrinkage (moving boundary) and microwave intermittency during the drying of food products employing a coupled pulsed microwave and hot air. This study aimed to establish a comprehensive model incorporating electromagnetic wave propagation, heat, and mass transfer to assess the uniformity of microwave-induced temperature and moisture distributions for enhancing food quality. Additionally, the interactive effects of varying microwave power levels and pulse ratios on key product and process parameters, including drying kinetics, drying rate, effective moisture diffusivity (D_{eff}), shrinkage, bulk density, rehydration ratio, and energy consumption, were systematically evaluated.

2. Materials and methods

2.1. Sample preparation

Potatoes (var. *Agria*) were purchased from a local store and stacked at 8 °C. To affirm consistency during the experimentations and lower trial errors, all potatoes were obtained from identical place and variety. The potatoes were washed, peeled, and cut into 6 cm diameter and 2 mm thick slices employing a cutter. To keep away from enzymatic browning, the potatoes were blanched in water at 90 °C using a 1:5 mass ratio (potato to water) for 2 min. Afterward, the samples were instantaneously cooled in water (5 °C) to abolish extra heat. The surface moisture of the samples was erased through absorbent paper (Dehghannya et al., 2019).

2.2. Drying experiments

The blanched potatoes were dried implementing a dual microwave and hot air dryer (LG SolarDOM, model SD-3855SCR, Korea), stocked with a rotating tray (2.5 rpm) (Fig. 1). In the first drying stage, the samples were subjected to microwave powers of 0 (control; hot air), 360, 600, and 900 W at pulse ratios of 1 (continuous), 2, 4, and 6. The microwave application ("on") times, concerning a constant "off" time (180 s) at different pulse ratios, were attained by Eq. (1) (Dehghannya et al., 2023a) and are presented in Table 1.

$$PR = \frac{t_{on} + t_{off}}{t_{on}} \quad (1)$$

where, PR denotes the pulse ratio (dimensionless), t_{on} represents the microwave "on" time (s), and t_{off} is the microwave "off" time (s).

The microwave "on" time was adjusted by trial and error, affirming maximum moisture exclusion without burning the potato samples. In the second drying stage, drying progressed with hot air at low temperature (40 °C) using an air velocity of 1 m/s up to the moisture hit 0.1 g water per g dry solids (Dehghannya et al., 2023b).

2.3. Measurement of quantitative and qualitative indices

2.3.1. Drying kinetics

To quantify the moisture content of the potatoes, they were positioned in an oven (model BM120, Fan Azma Gostar, Iran) at 105 °C for 24 h up to a stable mass was achieved. The moisture content was estimated by (Dehghannya et al., 2018a):

$$MC_{d.b.} = \frac{M_w}{M_s} \quad (2)$$

where, M_w represents the moisture mass (g), and M_s denotes the dry

solids mass (g).

2.3.2. Drying rate

The drying rate was derived by (Dehghannya et al., 2023a):

$$DR = \frac{M_t - M_{t+\Delta t}}{\Delta t} \quad (3)$$

where, DR designates the drying rate ($g_{water}/g_{dry\ solids}$·min), M_t and $M_{t+\Delta t}$ the moisture content at times t and $t + \Delta t$ ($g_{water}/g_{dry\ solids}$), and Δt the time interval (min).

2.3.3. Effective moisture diffusivity (D_{eff})

Diffusion is deemed the prime mechanism for moisture transfer during drying. The moisture ratio (MR) was attained through the Crank equation for an infinite plate (Emam-Djomeh et al., 2006):

$$MR = \frac{M_t - M_e}{M_0 - M_e} = \frac{8}{\pi^2}\sum_{n=1}^{\infty}\frac{1}{(2n-1)^2}\exp\left(-\frac{(2n-1)^2\pi^2 D_{eff}}{4L^2}\right)t \quad (4)$$

where, M_t symbolizes the moisture at time t ($g_{water}/g_{dry\ solids}$), M_0 the initial moisture ($g_{water}/g_{dry\ solids}$), M_e the equilibrium moisture ($g_{water}/g_{dry\ solids}$), "n" a positive integer, D_{eff} the effective moisture diffusivity (m^2/s), L the thickness of potato slice (mm), and "t" the process time (s).

For prolonged drying, the first term of the series in Eq. (4) is examined only. Moreover, since M_e is trivial compared to M_t and M_0, Eq. (4) simplifies to:

$$MR = \frac{M_t}{M_0} = \frac{8}{\pi^2}\exp\left(\frac{-\pi^2 D_{eff}}{4L^2}\right)t \quad (5)$$

By taking the natural logarithm, Eq. (6) becomes:

$$\ln(MR) = \ln\left(\frac{8}{\pi^2}\right) - \left(\frac{\pi^2 D_{eff}}{4L^2}\right)t \quad (6)$$

The D_{eff} can now be approximated from the slope of the ln (MR) against "t":

$$Slope = \frac{\pi^2 D_{eff}}{4L^2} \quad (7)$$

$$D_{eff} = \frac{Slope \times 4L^2}{\pi^2} \quad (8)$$

2.3.4. Shrinkage

The shrinkage was attained by (Dehghannya et al., 2023b):

$$Sh = \left(1 - \frac{V_t}{V_0}\right) \times 100 \quad (9)$$

where, V_0 denotes the initial sample volume (mm^3), and V_t represents the apparent sample volume after time t (mm^3).

To verify the apparent volume (V_t), the samples were weighed and put in a glass flask loaded in half with toluene. The remaining flask volume was filled up with toluene, and the whole mass was acquired. The V_t was estimated by:

$$V_t = V_f - \frac{M_{sf}}{\rho_s} \quad (10)$$

$$M_{sf} = M_{t+s} - M_f - M \quad (11)$$

where, V_f denotes the flask volume (cm^3), M_{sf} the toluene mass (g), M_{t+s} the flask, solvent, and sample mass (g), M_f the flask mass (g), M the sample mass (g), and ρ_s the toluene density (0.87 g/cm^3).

2.3.5. Bulk density

The bulk density was verified by (Dehghannya et al., 2023b):

$$\rho_b = \frac{m_t}{V_t} \quad (12)$$

where, ρ_b represents the bulk density (g/cm^3), m_t the product mass (g), and V_t the bulk volume (cm^3).

2.3.6. Rehydration ratio (RR)

To evaluate the RR, the potato samples were plunged into boiling water for 6 min. Extra water was removed with absorbent paper, and the potatoes were weighed. The RR was estimated by (Chen et al., 2020):

$$RR = \frac{M_h}{M_i} \quad (13)$$

where, M_h denotes the potatoes mass after rehydration (g), and M_i ascribes the dried potatoes mass (g).

2.3.7. Energy consumption

The total energy consumption (E) was estimated by (Dehghannya et al., 2023a):

$$E = E_1 + E_2 \quad (14)$$

where, E_1 assigns the energy consumed during the microwave drying (kJ/kg), and E_2 represents the energy consumed during the hot-air drying (kJ/kg).

To acquire the energy consumption of microwave (E_1) and hot air (E_2) drying stages, Eq. (15) and Eq. (16) were applied, respectively.

$$E_1 = \frac{Pt_m}{PR \times m_1} \quad (15)$$

where, P denotes the microwave power (W), t_m the microwave drying time (s), PR the pulse ratio, and m_1 the moisture mass abolished through microwaves (kg).

$$E_2 = \frac{AV_{air}\rho_{air} \times \Delta H \times t_c}{m_2} \quad (16)$$

where, A represents the container area holding the potatoes (m^2), V_{air} the airflow rate (m/s), ρ_{air} the air density (kg/m^3), ΔH the air enthalpy (kJ/kg dry air), t_c the hot-air drying time (s), and m_2 the moisture mass abolished through hot air (kg).

$$\Delta H = (Cp_{air} + WCp_v)(T_{in} - T_{amb}) + w\lambda \quad (17)$$

where, Cp_{air} assigns the air specific heat capacity (kJ/kg.K), W the air absolute humidity (kg water vapor/kg dry air), Cp_v the water vapor specific heat capacity (kJ/kg.K), T_{in} the dryer internal temperature (K), T_{amb} the ambient temperature (K), and λ the latent heat of evaporation (kJ/kg water vapor).

2.4. Statistical analysis

The statistical examinations were implemented by a 4 × 4 × 3 factorial experiment (4 microwave powers (0 (control: hot air), 360, 600, and 900 W), 4 pulse ratios (1 (continuous), 2, 4, and 6)) in triplicate, utilizing a completely randomized design to investigate the impacts of these variables on the characteristics of the samples during joint pulsed microwave and hot air drying. Mean comparisons were achieved employing Duncan's multiple range test at a 95% confidence level. Analysis of variance was performed in SAS software (version 9.4).

2.5. Mathematical modeling of electromagnetic waves, heat and mass transfer

2.5.1. Model assumptions

1) Initial consistent propagation of the electric field around the food.

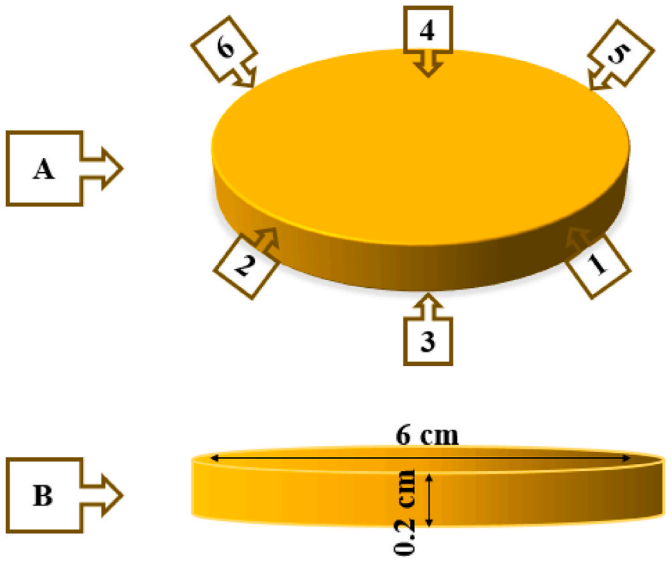

Fig. 2. 3D view of the model boundaries (A) and dimensions of the model (B) [The side boundaries are marked with numbers 1, 2, 5 and 6, the top surface boundary is marked with number 4, and the bottom surface boundary is marked with number 3].

Table 2
Effect of temperature on thermophysical properties of potato components.

Thermophysical property	Components	Temperature[a] dependent equation
Thermal conductivity coefficient (k; W/m.K)	Carbohydrate	$k = 0.20141 + 1.3874 \cdot 10^{-3} T - 4.3312 \cdot 10^{-6} T^2$
	Ash	$k = 0.32962 + 1.4011 \cdot 10^{-3} T - 2.9069 \cdot 10^{-6} T^2$
	Fiber	$k = 0.18331 + 1.2497 \cdot 10^{-3} T - 3.1683 \cdot 10^{-6} T^2$
	Fat	$k = 0.18071 + 2.7604 \cdot 10^{-4} T - 1.7749 \cdot 10^{-7} T^2$
	Protein	$k = 0.17881 + 1.1958 \cdot 10^{-3} T - 2.7178 \cdot 10^{-6} T^2$
	Water	$k = 0.57109 + 1.7625 \cdot 10^{-3} T - 6.7036 \cdot 10^{-6} T^2$
Density (ρ; kg/m^3)	Carbohydrate	$\rho = 1.5991 \cdot 10^3 - 0.31046 T$
	Ash	$\rho = 2.4238 \cdot 10^3 - 0.28063 T$
	Fiber	$\rho = 1.3115 \cdot 10^3 - 0.36589 T$
	Fat	$\rho = 9.2559 \cdot 10^2 - 0.41757 T$
	Protein	$\rho = 1.3299 \cdot 10^3 - 0.51840 T$
	Water	$\rho = 997.18 + 3.1439 \cdot 10^{-3} T - 3.7574 \cdot 10^{-3} T^2$
Specific heat at constant pressure (Cp; kJ/kg.K)	Carbohydrate	$Cp = 1.5488 + 1.9625 \cdot 10^{-3} T - 5.9399 \cdot 10^{-6} T^2$
	Ash	$Cp = 1.0926 + 1.8896 \cdot 10^{-3} T - 3.6817 \cdot 10^{-6} T^2$
	Fiber	$Cp = 1.8459 + 1.8306 \cdot 10^{-3} T - 4.6509 \cdot 10^{-6} T^2$
	Fat	$Cp = 1.9842 + 1.4733 \cdot 10^{-3} T - 4.8008 \cdot 10^{-6} T^2$
	Protein	$Cp = 2.0082 + 1.2089 \cdot 10^{-3} T - 1.3129 \cdot 10^{-6} T^2$
	Water	$Cp = 2.0082 + 1.2089 \cdot 10^{-3} T - 1.3129 \cdot 10^{-6} T^2$

[a] In all equations, the temperature (T) during at two stages of drying with microwaves (T_m) and hot air (T_a) were considered separately.

2) Initial consistent temperature and moisture inside the potatoes.
3) Moisture elimination by diffusive mechanism from inside to the surface of the potatoes.
4) Moisture evaporation by convective mechanism from surface to the adjacent environment.
5) Temperature-dependence of the potato thermophysical properties.

Table 3
Various parameters employed in the modeling.

Parameter	Value	Symbol	Reference
Initial temperature	25 [°C]	T_0	This study
Water molecular mass	0.018 [kg/mol]	M_{water}	Kumar et al. (Kumar et al., 2016)
Air moisture content	$0.02 \times \rho_P/M_{water}$ [mol/m^3]	c_{air}	Kumar et al. (Kumar et al., 2018)
Product initial moisture content	$5 \times \rho_P/M_{water}$ [mol/m^3]	c_0	This study
Latent heat of vaporization	2.3×10^6 [J/kg] × M_{water} [kg/mol]	L_{heat}	Kumar et al. (Kumar et al., 2016)
Drying air temperature	40 [°C]	T_{dry}	This study
Frequency	2.45 [GHz]	f	This study
Wavelength	0.122 [m]	λ	This study
Dielectric constant	64	ε'	Heshmati et al. (Heshmati et al., 2023)
Dielectric loss factor	14	ε''	Heshmati et al. (Heshmati et al., 2023)
Loss tangent	0.21875	tan δ	This study
Air density	1.096 [kg/m^3]	ρ_{air}	Pavón-Melendez et al. (Pavón et al., 2002)
Air dynamic viscosity	0.000019432	μ_{air}	Pavón-Melendez et al. (Pavón et al., 2002)
Air thermal conductivity coefficient	0.027516 [W/mK]	k_{air}	Pavón-Melendez et al. (Pavón et al., 2002)
Air specific heat	1007.8 [J/kgK]	Cp_{air}	Perussello et al. (Perussello et al., 2014)
Air effective mass diffusion coefficient	2.86612×10^{-5} [m^2/s]	D_{air}	Kumar et al. (Kumar et al., 2018)
Air thermal diffusion coefficient	2.50×10^{-5} [m^2/s]	α_{air}	Perussello et al. (Perussello et al., 2014)
Drying air velocity	1 [m/s]	V_{air}	This study
Product diameter	6 [cm]	D	This study
Product thickness	0.2 [cm]	L	This study
Product effective moisture diffusion coefficient	Table 6	D_{eff}	This study
Input microwave power	360, 600 and 900 [W]	P	This study

6) Constant D_{eff} throughout the drying process.

2.5.2. Model geometry

The geometry of the model was deemed as a planar surface (thickness: 2 mm and diameter: 6 cm), with its associated boundaries (Fig. 2).

2.5.3. Thermophysical characteristics of potatoes and modeling parameters

Thermal conductivity, specific heat at fixed pressure, and density are the critical thermophysical characteristics that should be assigned to the potato samples. Temperature-dependent thermophysical properties were denoted for each potato constituent, including carbohydrates, ash, fiber, fat, protein, and water, to secure more exact simulation data (Table 2) (Fricke and Becker, 2001). Additionally, along with USDA (United States Department of Agriculture) data, regarding that 100 g of a potato contains 77.7 g water, 17.5 g carbohydrates, 1.6 g fiber, 1.44 g protein, 0.7 g ash, and 0.09 g fat, the thermophysical properties of the potatoes were estimated by (Fricke and Becker, 2001):

$$k_{Potato} = \sum k_i x_i^v \quad (18)$$

$$\rho_{Potato} = \frac{1-\varepsilon}{\sum \left(\frac{x_i}{\rho_i}\right)} \quad (19)$$

$$Cp_{Potato} = \sum Cp_i x_i \quad (20)$$

where, x_i^v denotes the volumetric fraction of constituent i, and x_i represents the mass fraction of constituent i. x_i^v was estimated by (Fricke and Becker, 2001):

$$x_i^v = \frac{\frac{x_i}{\rho_i}}{\sum\left(\frac{x_i}{\rho_i}\right)} \quad (21)$$

Different parameters utilized in the modeling are presented in Table 3.

2.5.4. Modeling physics

The modeling of electromagnetic waves, heat, and mass transfer phenomena during dual microwave (first stage) and hot air (second stage) drying was developed as follows.

2.5.4.1. Pulsed microwave drying. The Maxwell, Fourier, and Fick equations were, respectively, applied to model microwaves, heat, and mass transfer (Kumar et al., 2016; Raj and Dash, 2021):

$$\nabla \times \mu_r^{-1}(\nabla \times E) - \frac{(2\pi f)^2}{c}(\varepsilon' - i\varepsilon'')E = 0 \quad (22)$$

$$\rho C_p \frac{\partial T_m}{\partial t} + \nabla \bullet (-k\nabla T_m) = Q_m \quad (23)$$

$$\frac{\partial c_m}{\partial t} + \nabla \bullet \left(-D_{eff}\nabla c_m\right) = 0 \quad (24)$$

where, E denotes the electric field intensity (V/m), μ_r the relative permeability, ε' the dielectric constant, ε'' the dielectric loss factor, j the imaginary part, ρ the product density (kg/m^3), C_p the product specific heat at fixed pressure (J/kg·K), T_m the temperature during microwave drying (K), k the product thermal conductivity (W/m·K), Q_m the heat source developed by microwaves (W/m^3), c_m the moisture concentration during microwave drying (mol/m^3), and D_{eff} the effective moisture diffusivity (m^2/s).

To modify the concentration unit from mol/m^3 to g water per g dry solid (dimensionless), c_m was multiplied by the water molecular mass and divided by the product density. The product thermal conductivity, specific heat, and density were deemed as a function of T_m concerning their various constituents including carbohydrates, ash, fiber, fat, protein, and water (Table 2) (Fricke and Becker, 2001).

The heat developed by microwaves, Q_m (W/m^3), was estimated by:

$$Q_m = Q_{rh} + Q_{ml} \quad (25)$$

where, Q_{rh} assigns the resistive loss (W/m^3), and Q_{ml} the magnetic loss (W/m^3). Microwave energy is translated to heat owing to electrical resistance (resistive loss). Moreover, magnetic loss denotes energy conversion in a material subjected to an alternating magnetic field. Since food products do not own magnetic properties, the heat developed by magnetic losses Q_{ml} is trivial and is ignored (Kumar et al., 2018).

The resistive loss was estimated by:

$$Q_{rh} = 0.5 \bullet J \bullet E^* \quad (26)$$

where, J represents the current density (A/m^2) and E* denotes the complex conjugate of E.

The current density was obtained by:

$$J = \sigma \bullet E = 2\pi f \varepsilon_0 \varepsilon'' \bullet E \quad (27)$$

where, σ signifies the electrical conductivity (S/m), f the microwave frequency (Hz), ε_0 the permeability in free space, and ε'' the dielectric loss factor.

Accordingly, Eq. (25) becomes (Kumar and Karim, 2019):

$$Q_m = \pi f \varepsilon_0 \varepsilon'' |E|^2 \quad (28)$$

2.5.4.2. Hot-air drying. The Fourier and Fick equations were utilized, respectively, for heat and mass transfer modeling during hot-air drying (Kumar et al., 2016):

$$\rho C_p \frac{\partial T_a}{\partial t} + \nabla \bullet (-k\nabla T_a) = 0 \quad (29)$$

$$\frac{\partial c_a}{\partial t} + \nabla \bullet \left(-D_{eff}\nabla c_a\right) = 0 \quad (30)$$

where, ρ denotes the product density (kg/m^3), C_p the product specific heat at fixed pressure (J/kg.K), T_a the temperature during the hot-air drying stage (K), k the product thermal conductivity (W/m.K), c_a the moisture concentration during hot-air drying stage (mol/m^3), and D_{eff} the effective moisture diffusivity (m^2/s).

To translate the concentration unit from mol/m^3 to g water/g dry solids (dimensionless), c_a was multiplied by the water molecular mass and divided by the product density. The product thermal conductivity, specific heat, and density were deemed as a function of T_a concerning its constituents including carbohydrates, ash, fiber, fat, protein, and water (Table 2) (Fricke and Becker, 2001).

2.5.5. Initial and boundary conditions

2.5.5.1. Electromagnetic waves. To estimate the electromagnetic wave propagation, the initial condition of $E_{int} = 0$ was employed. Correspondingly, the boundary condition (B.C.) of the perfect electric conductor (Eq. (31)) was used in boundary 3, and the port B.C. (Eq. (32)) was considered in other boundaries (Fig. 2) (Kumar et al., 2016):

$$n \bullet E = 0 \quad (31)$$

$$S = \frac{\int (E_{int} - E) \bullet E}{\int E \bullet E} \quad (32)$$

where, n. E assigns the electric field intensity in the normal direction (V/m), S the power per unit area (W/m^2), E_{int} the initial electric field intensity (V/m), and E the electric field intensity (V/m).

2.5.5.2. Heat transfer during microwave drying. To achieve the temperature distribution during microwave drying, the initial condition of $T_{int} = 25$ °C was considered, where T_{int} is the product initial temperature. Moreover, the temperature B.C. (Eq. (33)) was applied in boundary 3, and the heat flux B.C. (Eq. (34)) was used in other boundaries (Fig. 2) (Kumar et al., 2016):

$$T = T_m \quad (33)$$

$$n \bullet k\nabla T_m = h(T_{ext} - T_m) - Q_{ev} \quad (34)$$

where, T_m represents the temperature during microwave drying stage (K), k the product thermal conductivity (W/m.K), T_{ext} the air temperature inside the oven during microwave drying (K), and Q_{ev} the evaporative cooling (W/m^2).

The convective heat transfer coefficient (h) was estimated by (Perussello et al., 2014):

$$h = \frac{Nu \times k_{air}}{d} \quad (35)$$

where, *Nu* assigns the Nusselt number (dimensionless), k_{air} the air thermal conductivity (W/m.K), and d the product thickness (mm).

The *Nu* was approximated by:

$$Nu = 0.683 Re^{0.466}\ Pr^{0.33} \quad (36)$$

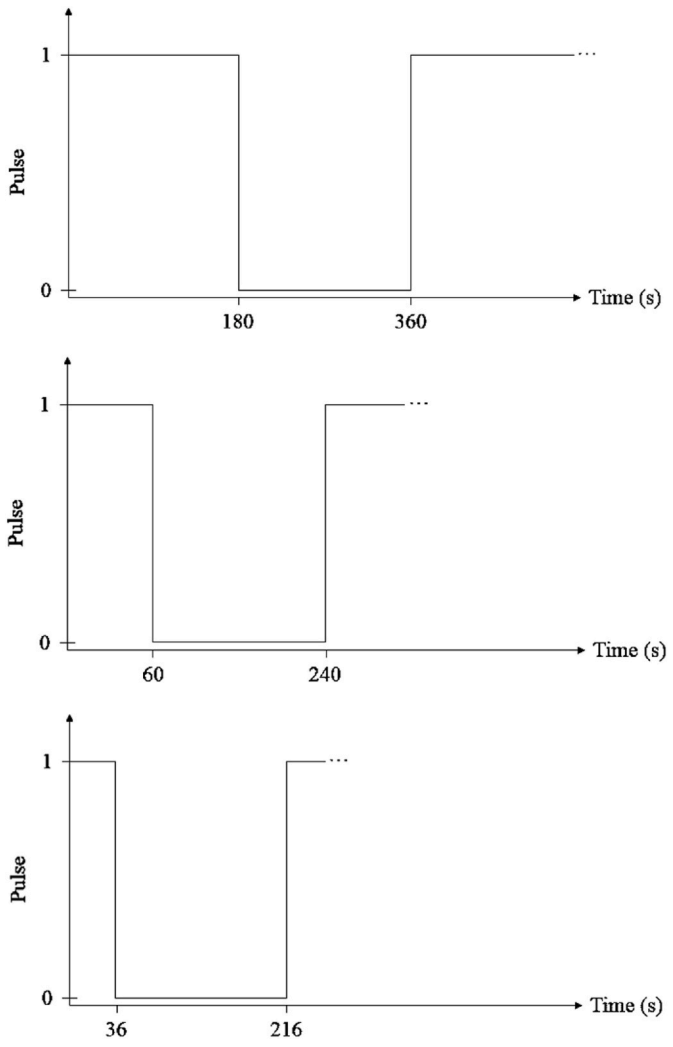

Fig. 3. The resulting graphs from Eq. (48), Eq. (49), and Eq. (50) for pulse ratios 2, 4 and 6, respectively, from top to bottom.

where, Re and Pr symbolize the dimensionless Reynolds and Prandtl numbers, respectively, estimated by (Pavón et al., 2002):

$$Re = \frac{\rho_{air} V_{air} d}{\mu_{air}} \tag{37}$$

$$Pr = \frac{Cp_{air} \mu_{air}}{k_{air}} \tag{38}$$

where, ρ_{air} denotes the air density (kg/m^3), V_{air} the air velocity (m/s), d the product thickness (mm), μ_{air} the air dynamic viscosity (Pa.s), Cp_{air} the air specific heat at fixed pressure (J/kg.K), and k_{air} the air thermal conductivity (W/m.K).

The evaporative cooling Q_{ev} was also estimated by:

$$Q_{ev} = \varphi \times k_c \times M_w (c_{air} - c_m) \tag{39}$$

where, φ signifies the latent heat of evaporation (J/kg), k_c the convective mass transfer coefficient (m/s), M_w the water molecular mass (kg/mol), c_{air} the air moisture content (mol/m^3), and c_m the product moisture content during microwave drying stage (mol/m^3).

2.5.5.3. Moisture transfer during microwave drying. To evaluate the moisture distribution during the microwave drying phase, the initial condition of $c_{int} = c_0$ was considered, where c_{int} is the initial product moisture, and c_0 is the product moisture at the start of drying. Also, the no flux B.C. (Eq. (40)) was applied in boundary 3, and the mass flux B.C. (Eq. (41)) was used in other boundaries (Fig. 2) (Kumar et al., 2016):

$$-n \bullet \left(-D_{eff} \nabla c_m\right) = 0 \tag{40}$$

$$-n \bullet \left(-D_{eff} \nabla c_m\right) = k_c (c_{air} - c_m) \tag{41}$$

where, D_{eff} assigns the effective moisture diffusivity (m^2/s), c_m the moisture concentration during microwave drying stage (mol/m^3), c_{air} the air moisture content (mol/m^3), and k_c the convective mass transfer coefficient (m/s).

The k_c was estimated by:

$$k_c = \frac{h}{\rho_{air} Cp_{air} \left(\frac{\alpha_{air}}{D_{air}}\right)^{2/3}} \tag{42}$$

where, h denotes the convective heat transfer coefficient (W/m^2.K), ρ_{air} the air density (kg/m^3), Cp_{air} the air specific heat at fixed pressure (J/kg.K), α_{air} the air thermal diffusivity (m^2/s), and D_{air} the air effective moisture diffusivity (m^2/s).

2.5.5.4. Heat transfer during hot air drying. To reach the temperature distribution during hot-air drying, the initial condition of $T_{int} = T_{fm}$ was considered, where T_{int} assigns the initial product temperature, and T_{fm} is the product temperature after completing the microwave drying stage and beginning the hot-air drying phase. Also, the temperature B.C. (Eq. (43)) was applied in boundary 3, and the heat flux B.C. (Eq. (44)) was utilized in other boundaries (Fig. 2) (Malafronte et al., 2012):

$$T_a = 40\ ^\circ C \tag{43}$$

$$n \bullet k \nabla T_a = h(T_{ext} - T_a) - Q_{ev} \tag{44}$$

where, T_a assigns the product temperature during hot-air drying stage (K), k the product thermal conductivity (W/m.K), T_{ext} the air temperature inside the oven during hot-air drying stage (K), and Q_{ev} the evaporative cooling (W/m^2).

The Q_{ev} was estimated by:

$$Q_{ev} = \varphi \times k_c \times M_w (c_{air} - c_a) \tag{45}$$

where, φ represents the latent heat of evaporation (J/kg), k_c the convective mass transfer coefficient (m/s), M_w the water molecular mass (kg/mol), c_{air} the air moisture content (mol/m^3), and c_a the product moisture content during hot-air drying stage (mol/m^3).

2.5.5.5. Moisture transfer during hot-air drying. To accomplish the moisture distribution during hot-air drying, the initial condition of $c_{int} = c_{fm}$ was used, where c_{int} assigns the initial product moisture content, and c_{fm} ascribes the product moisture content after finishing the microwave drying stage and beginning the hot-air drying phase. Also, the no flux B.C. (Eq. (46)) was applied in boundary 3, and the mass flux B.C. (Eq. (47)) was employed in other boundaries (Fig. 2) (Malafronte et al., 2012):

$$-n \bullet \left(-D_{eff} \nabla c_a\right) = 0 \tag{46}$$

$$-n \bullet \left(-D_{eff} \nabla c_a\right) = k_c (c_{air} - c_a) \tag{47}$$

where, D_{eff} assigns the effective moisture diffusivity (m^2/s), c_a the moisture concentration during the hot-air drying stage (mol/m^3), c_{air} the air moisture content (mol/m^3), and k_c the convective mass transfer coefficient (m/s).

2.5.6. Establishment of the periodic function

Periodic functions were allocated by utilizing analytic functions for the pulse ratios of 2, 4, and 6 (Eq. (48), Eq. (49), and Eq. (50)). The

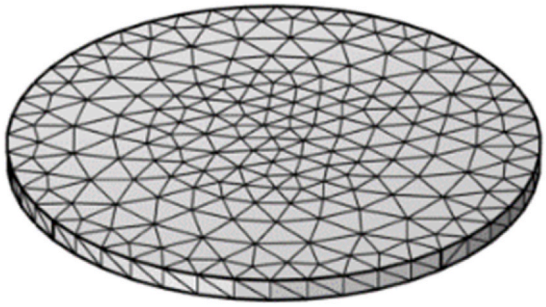

Fig. 4. "Fine" meshing structure employed in the modeling.

assigned functions were multiplied by the heat source, Q_m in the heat transfer physics for the first (microwave) drying stage (Eq. (23)) to regard the pulsed microwave drying (Kumar et al., 2016):

$$f(t) = \begin{cases} 1, n \le t \le n + 180 \\ 0, n + 180 < t < n + 360 \end{cases} \quad (48)$$

$$f(t) = \begin{cases} 1, n \le t \le n + 60 \\ 0, n + 60 < t < n + 240 \end{cases} \quad (49)$$

$$f(t) = \begin{cases} 1, n \le t \le n + 36 \\ 0, n + 36 < t < n + 216 \end{cases} \quad (50)$$

where, t assigns the drying time (s), and n varied from 0 to the whole microwave drying time (on + off times) considering the intervals 360, 240, and 216 for the pulse ratios 2, 4, and 6, respectively.

Fig. 3 demonstrates the graphs acquired from Eq. (48), Eq. (49), and Eq. (50).

2.5.7. Establishment of moving boundary

To employ the moving boundary (shrinkage), the deformed geometry procedure was utilized, and the shrinkage rate (m/s) at the product edges and top and bottom surfaces was achieved by (Aprajeeta et al., 2015):

$$v_{corners} = \frac{\Delta L}{t} \quad (51)$$

$$v_{top\ and\ bottom} = \frac{\Delta D}{t} \quad (52)$$

where, ΔL assigns the variation in height (m), ΔD the variation in diameter (m), and t the drying time (s). The deformed geometry physics with a normal mesh velocity B.C. was used to the product edge (lateral) boundaries and the top and bottom surfaces according to Eq. (51) and Eq. (52), respectively. The product diameter and thickness before and after drying were verified employing a caliper with an accuracy of 0.02 mm.

2.5.8. Numerical solution and model validation

The numerical solution for the simultaneous modeling of electromagnetic, heat, and mass transfer was done by COMSOL Multiphysics software employing the finite element method, considering mesh sensitivity examinations. For instance, Fig. 4 reveals the mesh

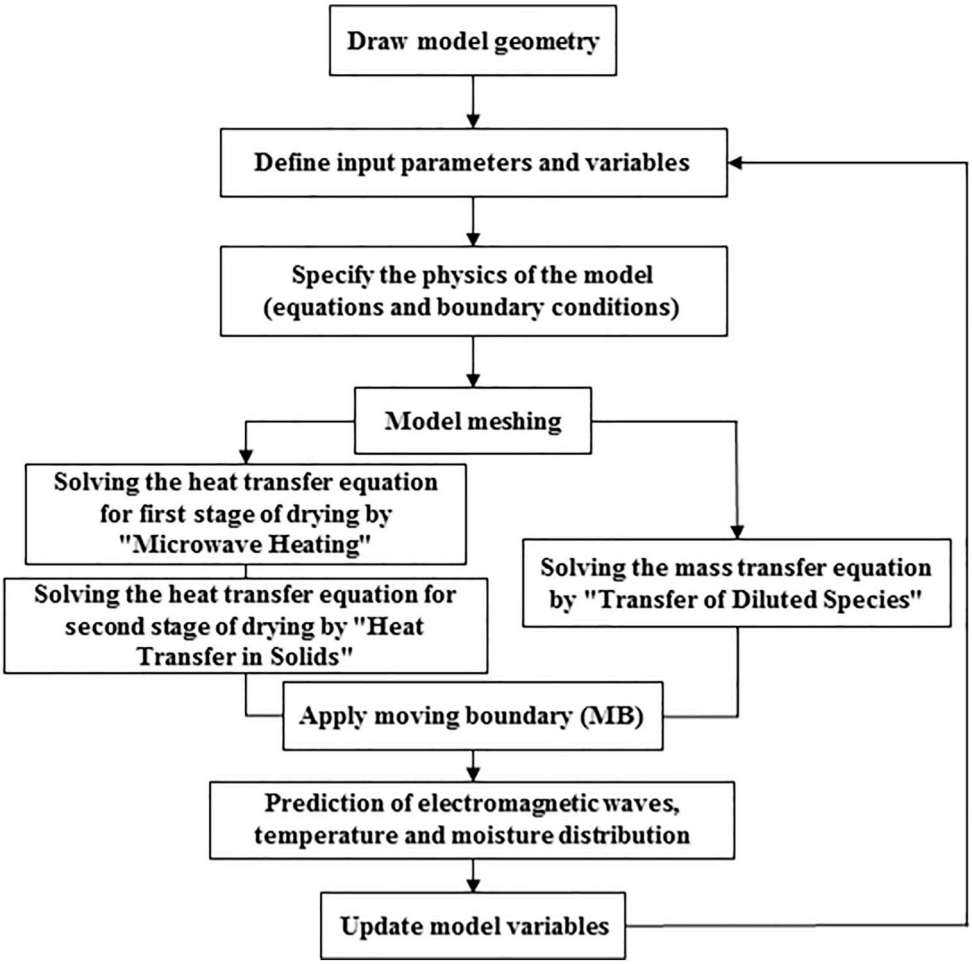

Fig. 5. Modeling steps during combined pulsed microwave and warm-air drying of potatoes.

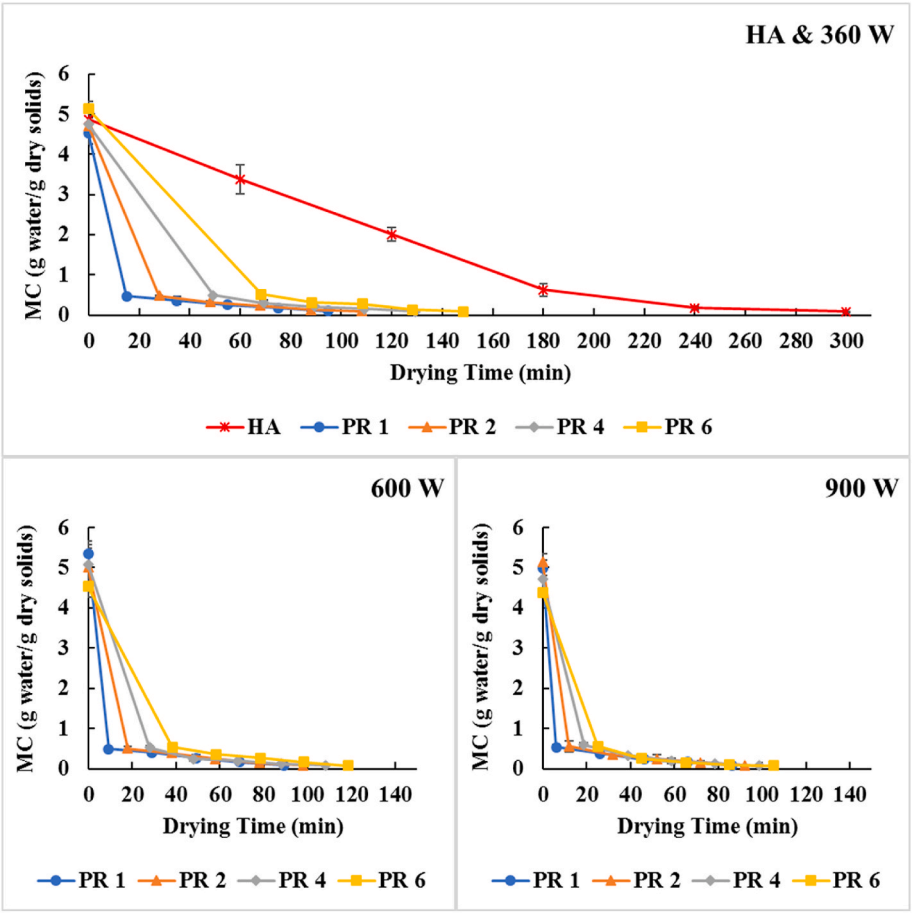

Fig. 6. Moisture content (MC) variation of potato samples during drying at microwave powers of 0 (HA), 360, 600 and 900 W and pulse ratios (PR) of 1, 2, 4 and 6.

development of the "Fine" type. The modeling phases during coupled microwave and hot-air drying are demonstrated in Fig. 5. The mass transfer model validation was performed explicitly by measuring the product moisture, followed by differentiating the experimental and predicted data using the RMSE and R^2 (Raj and Dash, 2021):

$$RMSE = \sqrt{\frac{\sum_{i=1}^{n}\left(y_{Sim} - y_{Exp}\right)^2}{n}} \quad (53)$$

$$R^2 = 1 - \frac{RSS}{TSS} = 1 - \frac{\sum_{i=1}^{n}\left(y_{Sim} - \overline{y}_{Sim}\right)^2}{\sum_{i=1}^{n}\left(y_{Exp} - \overline{y}_{Exp}\right)^2} \quad (54)$$

where, y_{Sim} denotes the simulated data, y_{Exp} the experimental data, n the number of observations, RSS the residual sum of squares, TSS the total sum of squares, and $\overline{y}$ the mean of the y values. The electromagnetic and heat transfer modeling validation was implicitly done by utilizing the validation achieved from the mass transfer modeling (Dehghannya et al., 2018c).

2.5.8.1. Interaction effect of power and pulse ratio on simulation parameters. The simulation of combined drying of potatoes, considering shrinkage (moving boundary), was executed at 360, 600, and 900 W with microwave pulse ratios of 1, 2, 4, and 6, hot air temperature of 40 °C, and air velocity of 1 m/s. In the simulations, thermophysical properties at different microwave (T_m) and hot air (T_a) stages were considered based on temperature for various pulse ratios (Table 2). Heat and mass transfer modeling were conducted to determine the distribution of temperature and moisture at 1-min intervals. For mesh independence analysis, sensitivity tests were performed for 360, 600, and 900 W with pulse ratios of 1, 2, 4, and 6 using Normal, Fine, and Finer meshes. No significant changes in electromagnetic waves, temperature, and moisture distributions were observed when refining the elements from Fine to Finer. Thus, the Fine mesh was chosen as the optimal setting with a maximum element size of 4.8, a minimum element size of 0.6, a maximum element growth rate of 1.45, a curvature factor of 0.5, and a resolution of narrow region of 0.6 as predefined parameters in COMSOL Multiphysics software. The average simulation time recorded for different power levels and pulse ratios was approximately 520 s on a 64-bit system with an Intel Core i5 CPU, up to 2.67 GHz, and 4 GB RAM, with degrees of freedom of 25827 (plus 9084 internal degrees of freedom) for the microwave stage and 21836 (plus 9084 internal degrees of freedom) for the hot air stage.

3. Results and discussion

3.1. Drying kinetics

Fig. 6 illustrates the impact of various powers and pulse ratios on the drying kinetics of potato samples over time. In these graphs, the gap between the first and second markers indicates the microwave drying stage (MW), and the second marker shows the start of the hot-air drying stage (HA). In all treatments, moisture content decreased over time, but this reduction had a steeper slope during the microwave stage compared to the hot air phase. This was associated with the significant impact of microwave energy on reducing moisture content. At the beginning of the drying, due to the substantial moisture and more free water, microwave energy is absorbed more efficiently, leading to rapid heating of the

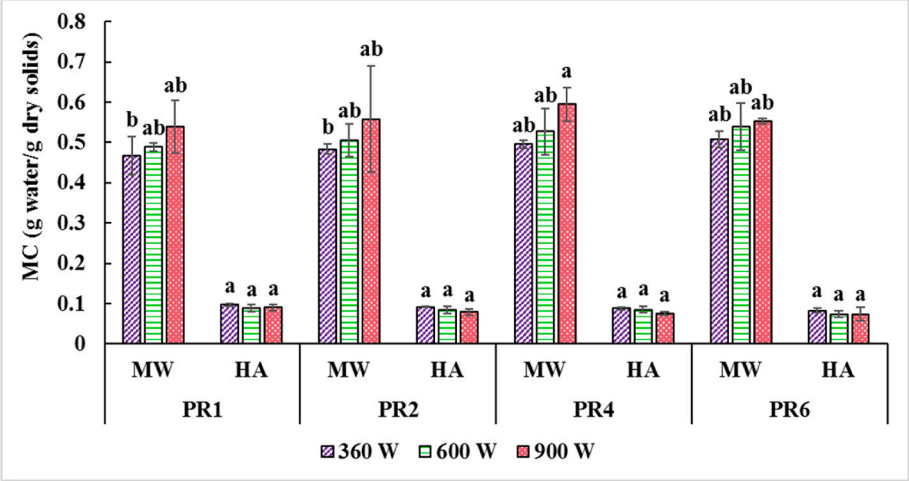

Fig. 7. Moisture content (MC) of potato samples after applying microwave (MW) and final moisture content after applying hot air (HA) at powers of 360, 600 and 900 W and pulse ratio (PR) of 1, 2, 4 and 6.

Table 4
Mean comparison of moisture content (MC; $g_{water}/g_{dry\ solids}$) after microwave (MW) drying, final MC ($g_{water}/g_{dry\ solids}$), microwave drying time (MW (on + off); min), drying time considering microwave "on" time and hot air (MW (on) + HA; min), and drying time considering microwave "on", microwave "off", and hot air times (MW (on + off) + HA; min) of potato slices as influenced by different process variables.

Process variable		MC after MW ($g_{water}/g_{dry\ solids}$)	Final MC ($g_{water}/g_{dry\ solids}$)	MW (on + off; min)	MW (on) + HA (min)	MW (on + off) + HA (min)
MW power (W)	**360**	0.488^{b}	0.090^{a}	40.183^{a}	93.182^{a}	120.183^{a}
	600	0.515^{b}	0.083^{b}	23.391^{b}	87.891^{b}	103.391^{b}
	900	0.561^{a}	0.079^{b}	15.508^{c}	85.256^{c}	95.508^{c}
MW pulse ratio	**1**	0.498^{a}	0.091^{a}	10.111^{d}	90.111^{a}	90.111^{d}
	2	0.515^{a}	0.085^{ab}	19.333^{c}	89.666^{a}	99.333^{c}
	4	0.539^{a}	0.083^{bc}	32^{b}	87.996^{b}	112^{b}
	6	0.533^{a}	0.076^{c}	44^{a}	87.333^{b}	124^{a}

Different letters in the same column for each variable indicate a significant difference ($p < 0.05$).

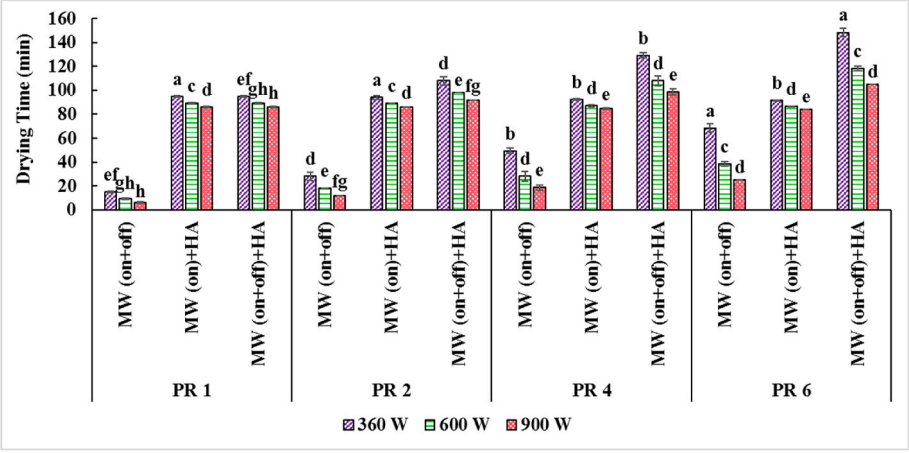

Fig. 8. Drying time considering microwave "on" and "off" time (MW (on + off)), drying time considering microwave "on" time and hot air (MW (on) + HA) and total drying time considering microwave "on" and "off" time and hot air (MW (on + off) + HA) at powers of 360, 600 and 900 W and pulse ratios (PR) of 1, 2, 4 and 6.

samples and further moisture reduction (Chatzilia et al., 2023). In the subsequent hot-air drying stage, due to the elimination of most surface moisture during the microwave stage and the reduction of free water, the moisture content gradually decreased to 0.1 g water per g dry solids.

Fig. 7 shows the moisture content of the samples after the first (MW) and second (HA) drying stages at various powers and pulse ratios. Overall, the moisture content in the microwave stage increased with higher power across all pulse ratios (Table 4). This result can be attributed to increased microwave energy, resulting in higher temperatures, enhanced heating of the product, and reduced drying time by microwaves (Table 4) (Dehghannya et al., 2023b). In contrast, in the hot air stage, moisture content decreased with increased power across all pulse ratios (Table 4). At higher power levels, due to increased vapor pressure and reduced structural damage, moisture removal in the hot air stage was facilitated (Kumar et al., 2018). Similar trends were observed in Kumar et al. (2018) and Dehghannya et al. (2023b).

On the other hand, the increase in pulse ratio led to higher moisture content during the microwave stage across all applied power levels

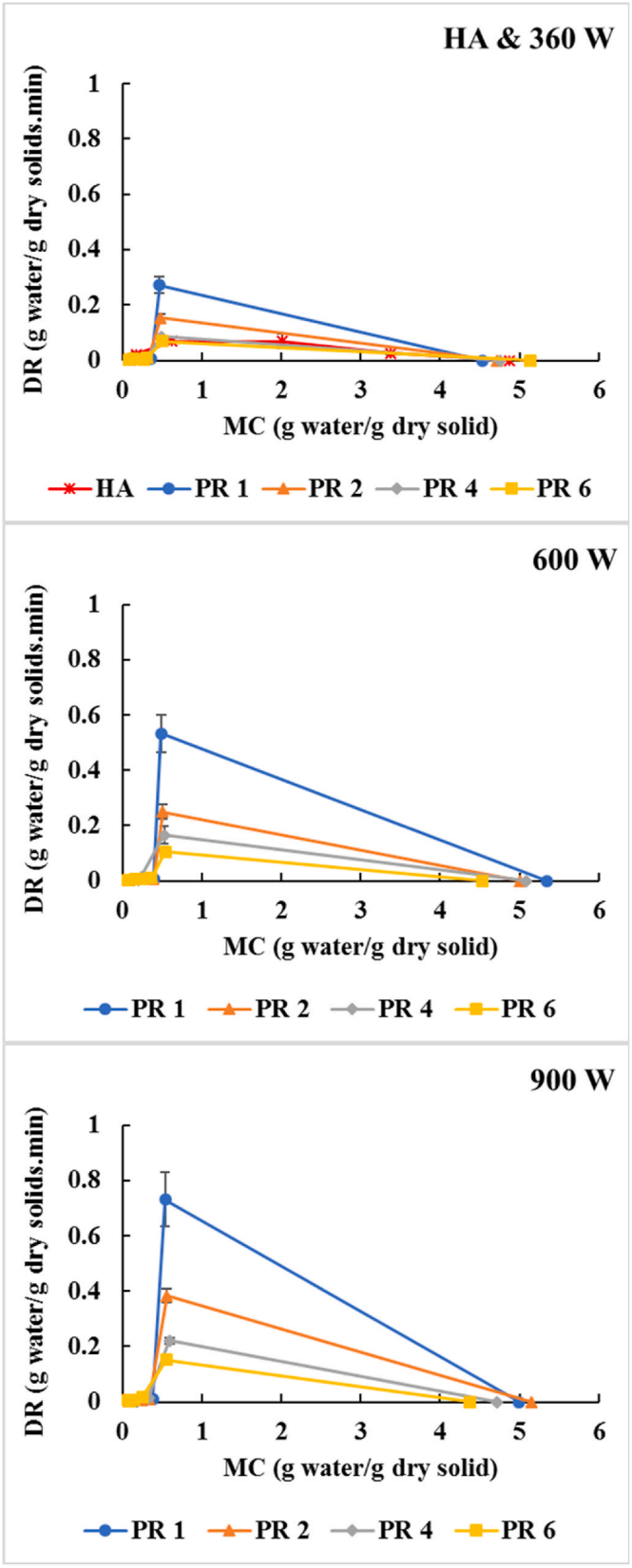

Fig. 9. Drying rate (DR) variation of potato samples during drying at microwave powers of 0 (HA), 360, 600 and 900 W and pulse ratios (PR) of 1, 2, 4 and 6.

(Table 4). This could be due to the reduced microwave exposure ("on") time during the fixed off-time (180 s) (Table 1), which subsequently reduced moisture removal. Conversely, in the hot air stage, moisture content decreased with a rise in pulse ratio (Table 4). This outcome was attributed to the reduced shrinkage (increased porosity) (section 3.4) and better preservation of the potato's vascular tissues at higher pulse ratios, leading to more efficient heat dissipation during the hot air stage (Pham et al., 2018). A similar trend was observed in Dehghannya et al. (2023a). Furthermore, the results indicated that the moisture content of the control treatment (hot air only) showed a milder slope and a longer drying time (300 min) compared to other treatments due to the application of low temperature (40 °C) and the need to heat the surrounding environment (Fig. 6) (Chen et al., 2020).

Fig. 8 illustrates the drying times of different treatments under three conditions: microwave on/off times, microwave on-times plus hot air, and microwave on/off times plus hot air. In general, the results showed that the total drying time significantly decreased by 20.53% with increased microwave power (Table 4). Due to the intensified electromagnetic field at higher microwave power, more heating occurred in the product, reducing the heating time (Table 4) (Huang et al., 2021). The entire drying time, regarding both microwave on and off times, increased by 37.61% with higher pulse ratios due to more cycles and consequently more off-times (Table 1). Conversely, drying time with increased pulse ratio during microwave on-times decreased, which can be attributed to reduced microstructural damage due to shorter microwave on-times (Table 1), leading to faster moisture removal during the hot air stage (Dehghannya et al., 2023b). These findings were in line with the studies of Pham et al. (2018), Huang et al. (2021), and Chatzilia et al. (2023).

Overall, the shortest and longest drying times among different treatments were observed at 900 W with a pulse ratio of 1 and 360 W with a pulse ratio of 6, respectively. Ultimately, the drying time of the control treatment (HA) was considerably prolonged (300 min) due to the use of low-temperature hot air, the need to heat the environment during hot air drying, and, consequently, the slower moisture removal rate (Fig. 6).

3.2. Drying rate

Fig. 9 illustrates the effect of power and pulse ratio on the drying rate of potato samples as a function of moisture content. The drying rate of all treatments reached its maximum during the microwave phase, due to the significant reduction in moisture content during this stage (Table 4). Subsequently, in the hot air phase, the drying rate showed a noticeable decline, which can be attributed to the reduced availability of surface water in the microwave stage, consequently lowering the moisture expelled in the hot air phase, and also the low temperature (40 °C) during this stage (Huang et al., 2021).

Fig. 10 shows the drying rate of potato samples after the first (MW) and second (HA) stages of drying at various powers and pulse ratios. As microwave power increased, the drying rate during the microwave stage had a steeper slope (Fig. 9), with a significant increase of 157.27% (Table 5). This was consistent with Dehghannya et al. (2021) and Huang et al. (2021). This effect can be attributed to better structural preservation at higher power levels, increased porosity (puffing), and consequently, higher moisture removal rates and mass transfer due to enhanced heat transfer (Dehghannya et al., 2023b). During the hot air stage, the drying rate also increased with higher power levels (Table 5). This result can be attributed to reduced structural damage and extended pore formation at higher microwave powers, facilitating moisture removal during the hot air stage (Dehghannya et al., 2023b).

Furthermore, Fig. 10 shows that the drying rate during the microwave and hot air stages decreased and increased, respectively, with higher pulse ratios, with a significant decrease of 78.93% in the microwave stage (Table 5). This result can be explained by the lower temperature increase during shorter on-times of the microwaves with

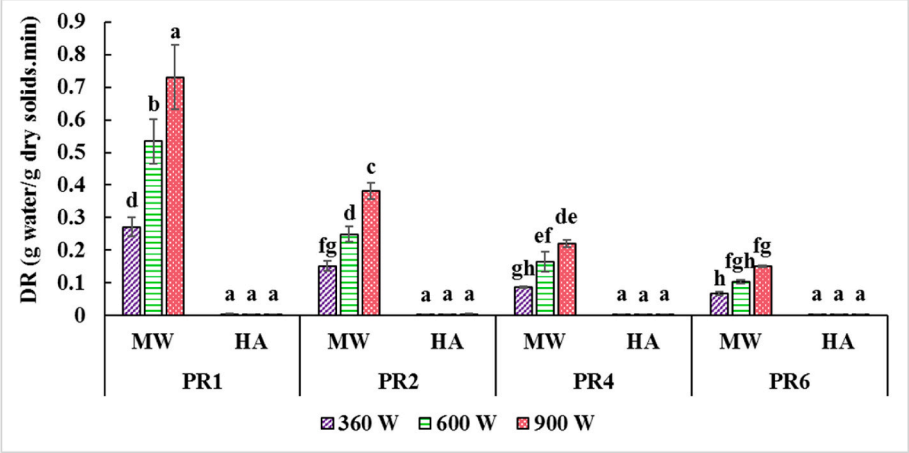

Fig. 10. Drying rate (DR) of potato samples in the microwave (MW) and hot air (HA) stage at the powers of 360, 600 and 900 W and pulse ratios (PR) of 1, 2, 4 and 6.

Table 5
Mean comparison of drying rate (DR; g water/g dry solids.min) after microwave (MW) drying and drying rate after hot-air (HA) drying of potato slices as influenced by various process variables.

Process variable		DR after MW	DR after HA
MW power (W)	**360**	0.1444^{c}	0.0026^{a}
	600	0.2631^{b}	0.0031^{a}
	900	0.3715^{a}	0.0034^{a}
MW pulse ratio	**1**	0.5117^{a}	0.0028^{a}
	2	0.2615^{b}	0.0027^{a}
	4	0.1576^{c}	0.0029^{a}
	6	0.1078^{c}	0.0038^{a}

Different letters in the same column for each variable indicate a significant difference ($p < 0.05$).

fixed off-times (Table 1), which subsequently led to reduced moisture removal. This finding was consistent with Pham et al. (2018) and Dehghannya et al. (2023a). On the other hand, the drying rate of the control treatment showed lower values (Fig. 9), which could be due to the longer drying time of hot air alone compared to other treatments (Fig. 6) (Dehghannya et al., 2018b).

3.3. Effective moisture diffusion coefficient (D_{eff})

Fig. 11 presents the ln (MR) values against drying time for potato samples at various powers and pulse ratios. The ln (MR) values for all treatments declined (negative slope) with drying time. Generally, the slope of the ln (MR) graph against drying time is directly related to D_{eff} (Eq. (8)). Table 6 presents the D_{eff} values under different power and pulse ratio levels. D_{eff} intensified by 6.07% and 10.57% with increasing power from 360 to 600 and 900 W, respectively, across various pulse ratios (Table 7). This result aligns with the findings of Chen et al. (2020), Huang et al. (2021), and Chatzilia et al. (2023). The increase in D_{eff} with higher power levels can be attributed to the enhanced motion of water dipoles and their increased collisions with microwaves, leading to more volumetric heating and easier moisture migration to the sample surface. Additionally, increased internal vapor pressure can help keep pores open, enhancing moisture diffusion and thus increasing D_{eff} (Chatzilia et al., 2023).

Moreover, the results showed that D_{eff} increased with rising pulse ratios across different power levels (Tables 6 and 7). This was linked to shorter microwave on-times at increased pulse ratios (Table 1), which reduced microstructural damage, preserved capillary structures better, and facilitated moisture removal during the hot air phase. A similar trend was observed in Dai et al. (2019). Overall, the highest and lowest D_{eff} values were observed in the treatments with 900 W and pulse ratio 6, and 360 W with pulse ratio 1 (after the control treatment), respectively (Table 6). The simultaneous rise in microwave power and pulse ratio led to a significant 14.28% intensification in D_{eff} (Table 6). This outcome can be attributed to the advantageous impact of increased power and pulse ratio on maintaining the microstructure and accelerating moisture transfer. In contrast, D_{eff} in the control treatment was the lowest among all treatments, which could be due to the low slope of the ln (MR) curve versus drying time (Fig. 11) and the extended drying duration (Fig. 6) (Chen et al., 2020).

3.4. Shrinkage

The results showed that shrinkage was notably high during the first drying phase (MW), as evidenced by the steeper graph slope (Fig. 12). However, shrinkage decreased in the second drying phase (HA) due to the lower temperature (40 °C) in this stage (Dehghannya et al., 2023b). The shrinkage of agricultural products such as potatoes during drying is influenced by their internal vapor pressure, which can be linked to the porous nature of these food materials.

Table 6 presents the shrinkage values of potatoes at different power and pulse ratio levels. Shrinkage decreased significantly by 16.56% with an increase in power from 360 to 900 W (Table 7). This was consistent with Dehghannya et al. (2021) and Heshmati et al. (2023). The reduction in shrinkage at higher power levels can be attributed to less structural damage due to shorter processing times resulting from increased heating within the product and enhanced porosity due to better structural preservation and increased internal vapor pressure (Chayjan et al., 2015). The results also indicated that shrinkage significantly decreased at higher pulse ratios, with a 12.4% reduction observed from pulse ratio 1 to 6 (Table 7). Dehghannya et al. (2023b) also reported that shrinkage in red beet samples decreased by 8.2% when the pulse ratio increased from 2 to 6. This could be due to uniform heat and moisture distribution within the product with reduced microwave on-times (Table 1), leading to accelerated moisture removal, better microstructure preservation, and increased porosity (Dehghannya et al., 2020).

Overall, the highest and lowest shrinkage values were observed in the treatments with 360 W and pulse ratio 1 (after the control treatment) and 900 W with pulse ratio 6, respectively (Table 6). Shrinkage decreased significantly by 26.28% with the concurrent increase in power and pulse ratio, due to the positive effects of higher power and pulse ratios on maintaining sample microstructure. The control treatment exhibited the highest shrinkage among all treatments (Fig. 12), which can be attributed to the extended drying time (Fig. 6) and, consequently, more substantial microstructural damage and lower porosity (Chen et al., 2020). The observed reduction in shrinkage with increasing microwave power and pulse ratio, compared to the control

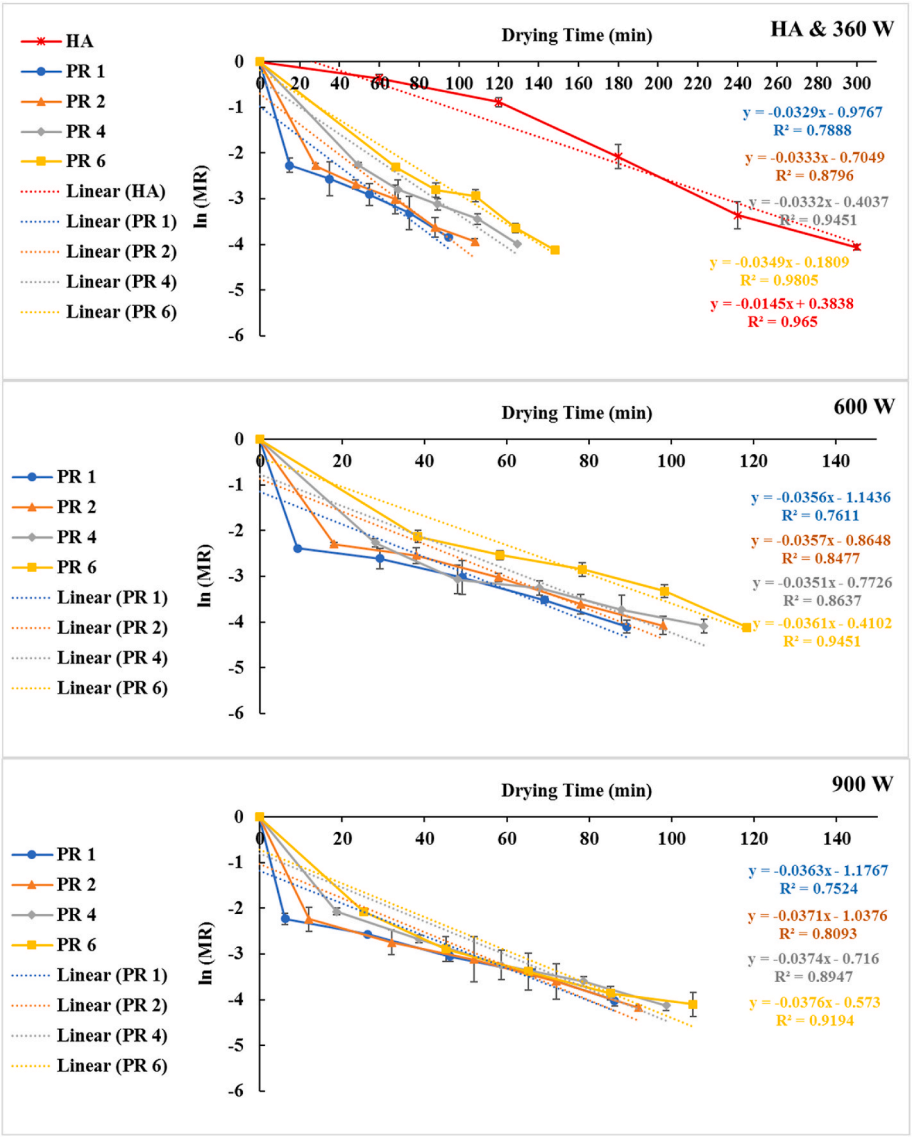

Fig. 11. Ln (MR) variation of potato samples during drying at microwave powers of 0 (HA), 360, 600 and 900 W and pulse ratios (PR) of 1, 2, 4 and 6.

Table 6
Effective moisture diffusion coefficient (D_{eff}; m^2/s), shrinkage (Sh; %), bulk density (ρ_b; g/cm^3), and rehydration ratio (RR; dimensionless) of potato slices as influenced by different microwave power (P; W) and pulse ratio (PR; dimensionless).

P	PR	D_{eff}	Sh	ρ_b	RR
360	1	$5.330 \times 10^{-8c} \pm 1.443 \times 10^{-9}$	$36.867^{b} \pm 0.188$	$0.121^{bcd} \pm 0.006$	$3.177^{f} \pm 0.032$
360	2	$5.390 \times 10^{-8bc} \pm 2.369 \times 10^{-9}$	$35.862^{bc} \pm 0.284$	$0.121^{bcd} \pm 0.005$	$3.254^{ef} \pm 0.009$
360	4	$5.381 \times 10^{-8bc} \pm 7.155 \times 10^{-10}$	$34.683^{cd} \pm 0.581$	$0.120^{bcd} \pm 0.005$	$3.367^{e} \pm 0.046$
360	6	$5.661 \times 10^{-8abc} \pm 2.389 \times 10^{-9}$	$33.166^{de} \pm 0.927$	$0.110^{cd} \pm 0.025$	$3.509^{d} \pm 0.209$
600	1	$5.785 \times 10^{-8abc} \pm 1.583 \times 10^{-9}$	$35.006^{c} \pm 0.697$	$0.123^{bc} \pm 0.005$	$3.243^{ef} \pm 0.055$
600	2	$5.789 \times 10^{-8abc} \pm 3.453 \times 10^{-9}$	$34.609^{cd} \pm 2.386$	$0.128^{b} \pm 0.005$	$3.347^{e} \pm 0.323$
600	4	$5.703 \times 10^{-8abc} \pm 3.357 \times 10^{-9}$	$32.749^{ef} \pm 0.409$	$0.117^{bcd} \pm 0.001$	$3.686^{c} \pm 0.079$
600	6	$5.807 \times 10^{-8abc} \pm 9.504 \times 10^{-9}$	$31.371^{f} \pm 1.404$	$0.105^{d} \pm 0.041$	$3.871^{b} \pm 0.131$
900	1	$5.890 \times 10^{-8abc} \pm 4.611 \times 10^{-10}$	$32.828^{ef} \pm 2.572$	$0.125^{bc} \pm 0.013$	$3.855^{b} \pm 0.035$
900	2	$6.019 \times 10^{-8ab} \pm 2.768 \times 10^{-9}$	$29.236^{g} \pm 0.526$	$0.120^{bcd} \pm 0.013$	$3.896^{b} \pm 0.025$
900	4	$6.064 \times 10^{-8a} \pm 7.782 \times 10^{-10}$	$28.063^{gh} \pm 1.294$	$0.118^{bcd} \pm 0.017$	$3.959^{b} \pm 0.091$
900	6	$6.091 \times 10^{-8a} \pm 3.639 \times 10^{-9}$	$27.179^{h} \pm 0.405$	$0.115^{bcd} \pm 0.049$	$4.097^{a} \pm 0.090$
Hot air (control)		$2.353 \times 10^{-8d} \pm 1.156 \times 10^{-9}$	$45.054^{a} \pm 0.384$	$0.145^{a} \pm 0.004$	$2.644^{g} \pm 0.130$

Different letters in the same column for each variable indicate a significant difference ($p < 0.05$).

Table 7
Mean comparison of effective moisture diffusion coefficient (D_{eff}; m^2/s), shrinkage (Sh; %), bulk density (ρ_b; g/cm^3), rehydration ratio (RR; dimensionless) and specific energy consumption (SEC; GJ/kg) of potato slices as influenced by different microwave (MW) process variables.

Process variable		D_{eff}	Sh	ρ_b	RR	SEC
MW power (W)	**360**	5.441×10^{-8c}	35.145^{a}	0.120^{a}	3.327^{c}	60.608^{a}
	600	5.771×10^{-8b}	33.434^{b}	0.118^{a}	3.537^{b}	59.283^{a}
	900	6.016×10^{-8a}	29.326^{c}	0.117^{a}	3.952^{a}	58.548^{a}
MW pulse ratio	**1**	5.668×10^{-8a}	34.900^{a}	0.124^{a}	3.425^{c}	68.202^{a}
	2	5.733×10^{-8a}	33.236^{b}	0.123^{a}	3.499^{c}	65.954^{a}
	4	5.716×10^{-8a}	31.832^{c}	0.118^{ab}	3.671^{b}	54.929^{b}
	6	5.853×10^{-8a}	30.572^{d}	0.110^{b}	3.826^{a}	48.833^{c}

Different letters in the same column for each variable indicate a significant difference ($p < 0.05$).

treatment, was corroborated by the moisture and temperature profiles obtained from simulation results (Section 3.9).

3.5. Bulk density

The bulk density decreased more sharply in the microwave stage than in the hot air stage (Fig. 13), which was attributed to the significant drop in moisture content during the microwave phase (Table 4). Generally, changes in bulk density depend on drying circumstances and structural alterations like shrinkage and porosity (Rodríguez-Ramírez et al., 2012).

Table 6 presents the bulk density values of potato samples under different power levels and pulse ratios. The bulk density decreased with increasing power across different pulse ratios (Table 7). Dehghannya et al. (2020) also obtained similar results. This outcome was due to the increased heat generated by microwaves at higher power levels, resulting in faster moisture removal and a more significant reduction in moisture content. Additionally, higher microwave power levels accelerated the drying process (Table 4), leading to reduced shrinkage (Table 6) and consequently, lower bulk density (Ali et al., 2023). Moreover, the results showed that bulk density decreased significantly by 11.29% with increasing pulse ratio from 1 to 6 across different power levels (Table 7). This decrease can be attributed to the shorter "on" time of microwaves during fixed "off" intervals (Table 1), promoting uniform heat distribution, minimizing shrinkage, and enhancing porosity (Dehghannya et al., 2023a, 2023b).

Overall, bulk density decreased significantly by 13.22% with the concurrent increase in power and pulse ratio (Table 6). On the other hand, the control treatment exhibited the highest bulk density among all treatments, which could be due to more significant structural damage caused by the extended drying time (300 min) (Fig. 6).

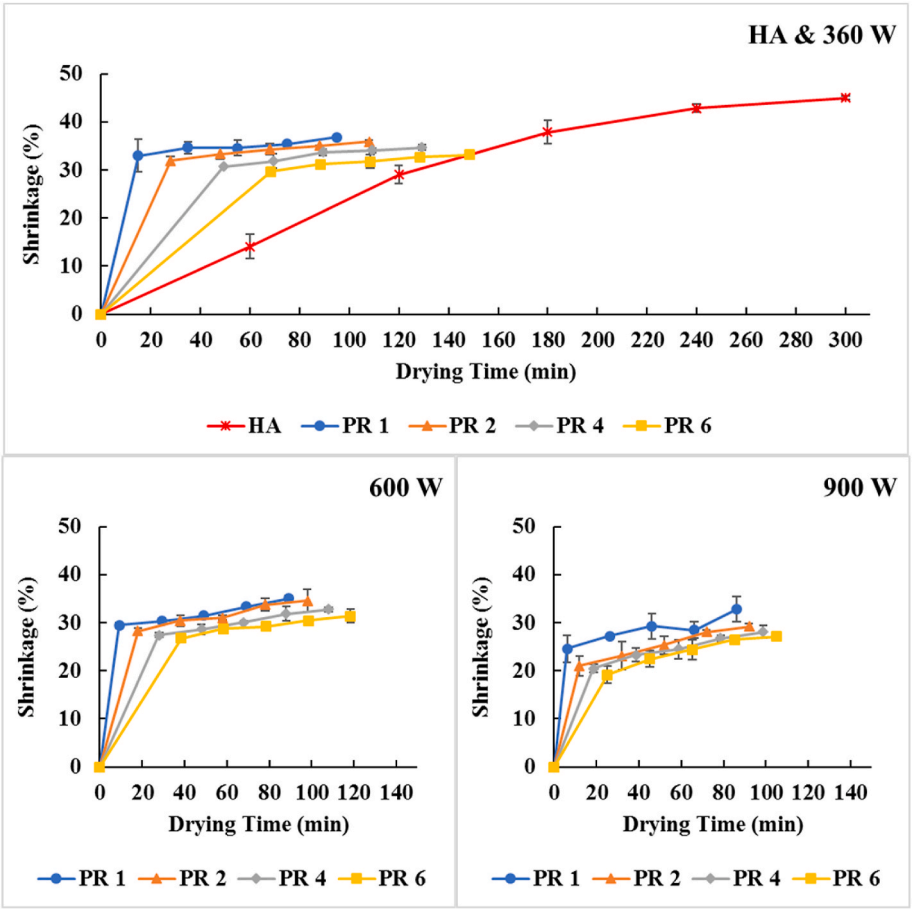

Fig. 12. Shrinkage variation of potato samples during drying at microwave powers of 0 (HA), 360, 600 and 900 W and pulse ratios (PR) of 1, 2, 4 and 6.

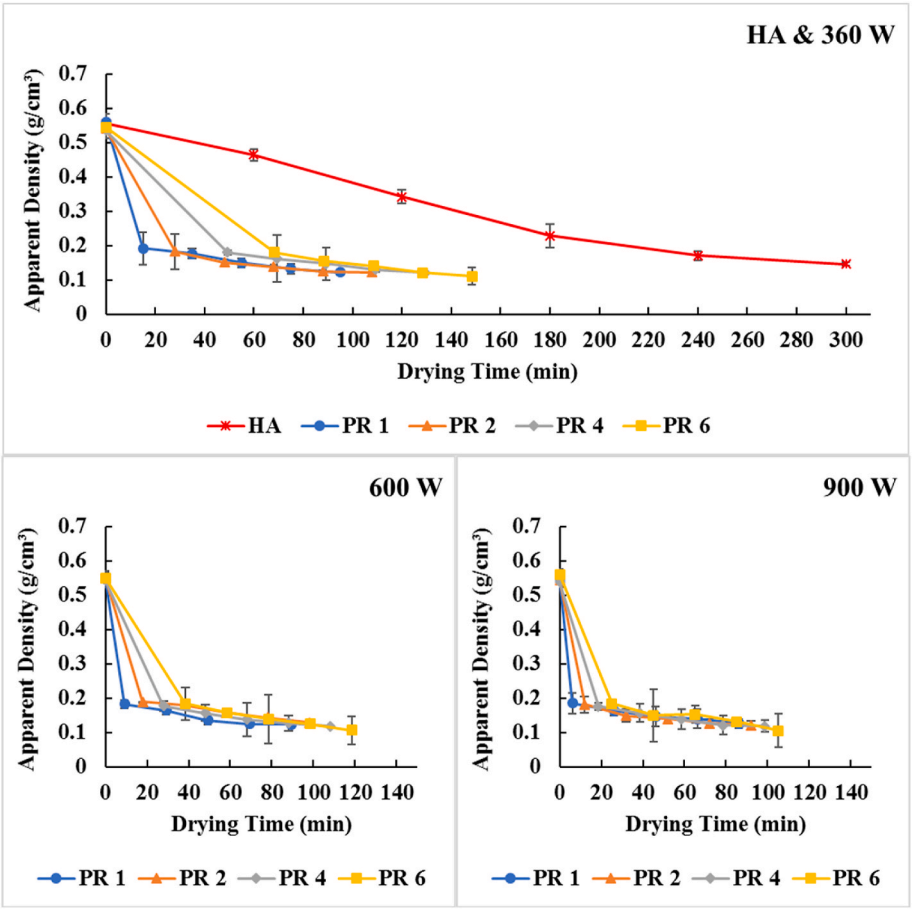

Fig. 13. Apparent density variation of potato samples during drying at microwave powers of 0 (HA), 360, 600 and 900 W and pulse ratios (PR) of 1, 2, 4 and 6.

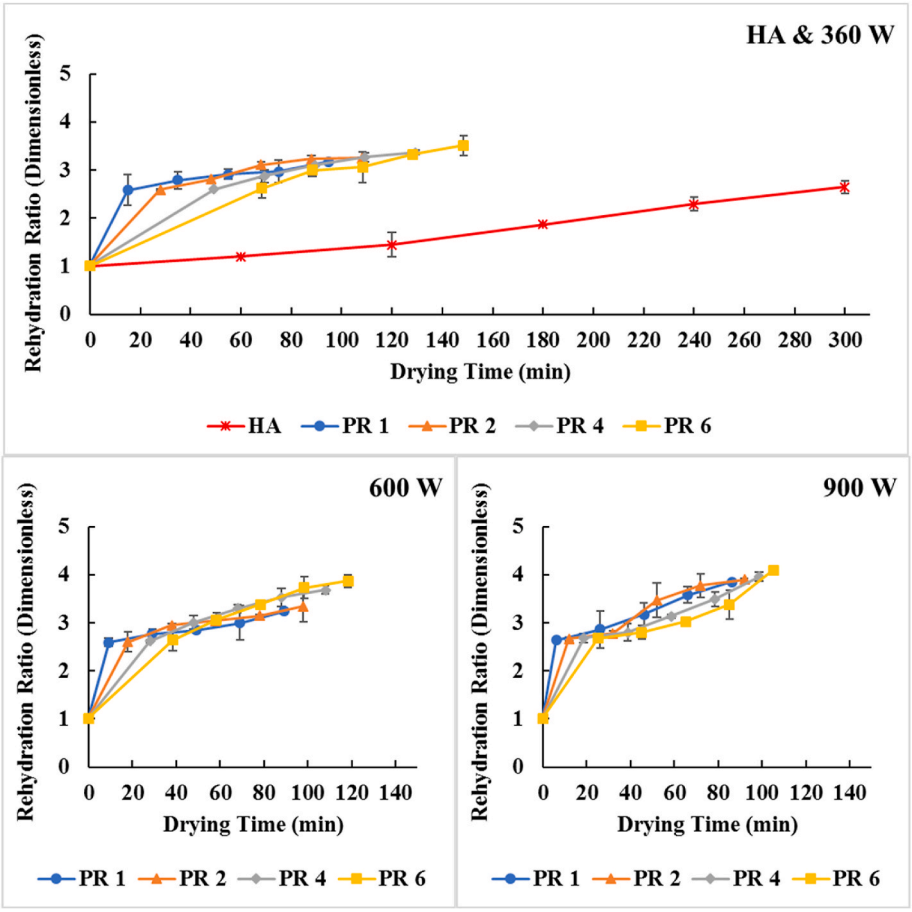

Fig. 14. Rehydration ratio variation of potato samples during drying at microwave powers of 0 (HA), 360, 600 and 900 W and pulse ratios (PR) of 1, 2, 4 and 6.

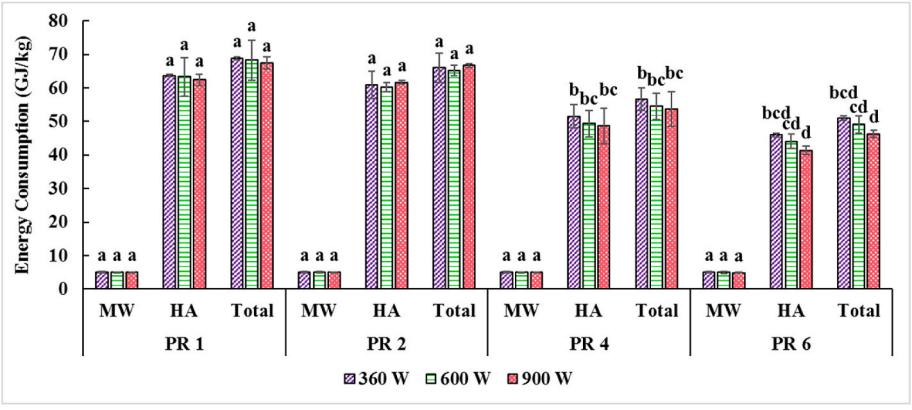

Fig. 15. Specific energy consumption of microwave (MW), hot air (HA) and microwave plus hot air (Total) for drying potato samples at powers of 360, 600 and 900 W and pulse ratios (PR) of 1, 2, 4 and 6.

3.6. Rehydration ratio

The results showed that rehydration ratio increased more in the first drying stage (MW) compared to the second stage (HA) (Fig. 14), due to the more considerable reduction in moisture content during the microwave stage (Table 4) (Chen et al., 2020). The extent of rehydration ratio during the drying process can be affected by the physicochemical changes in the sample, and complete rehydration ratio is not possible due to the irreversible collapse of the structure (Dehghannya et al., 2023a; Song et al., 2024).

Table 6 provides the rehydration ratio values of potato samples under different power levels and pulse ratios. Rehydration ratio increased significantly by 18.79% with rising power from 360 to 900 W (Table 7). This result was consistent with the findings of Ali et al. (2023) and Macedo et al. (2024). This increase can be due to the reduced drying time and better preservation of microstructure, leading to a more extensive pore structure, less damage to capillaries, and easier movement of water within them (Song et al., 2024). Furthermore, the rehydration ratio increased intensified by 11.71% as the pulse ratio increased from 1 to 6 (Table 7). A similar trend was observed in Dehghannya et al. (2023b), where increasing the pulse ratio from 2 to 6 led to a 19% significant increase in the rehydration ratio in red beet

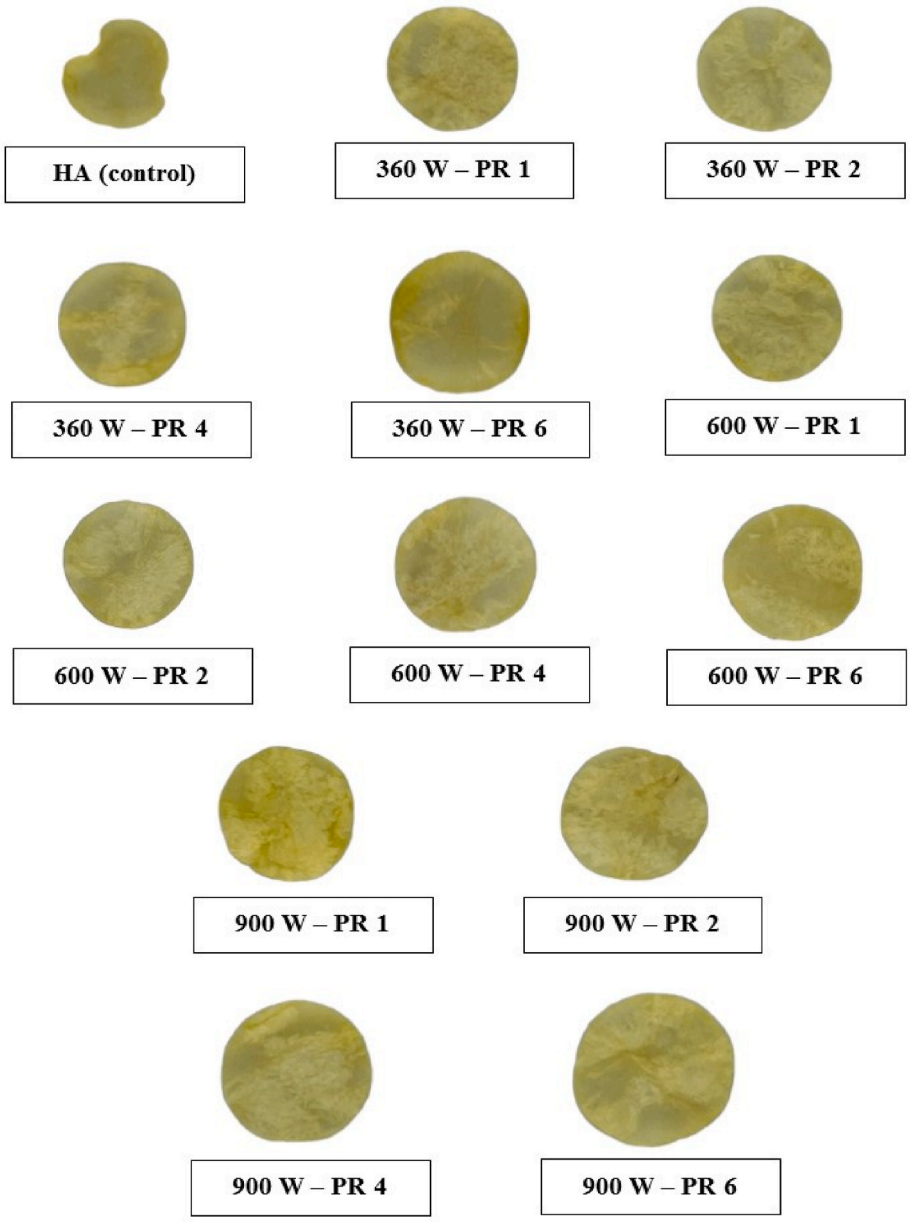

Fig. 16. Appearance of potato chips dried at microwave powers of 0 (HA), 360, 600 and 900 W and pulse ratios of 1, 2, 4 and 6.

Table 8
Different treatments assessed in the modeling for various microwave power (W) and pulse ratio (dimensionless).

Treatment	Microwave power	Microwave pulse ratio
1	0	0
2	360	1
3	360	2
4	360	4
5	360	6
6	600	1
7	600	2
8	600	4
9	600	6
10	900	1
11	900	2
12	900	4
13	900	6

samples. This was attributed to the reduced microwave “on” time with higher pulse ratios during fixed "off" periods (Table 1), reduced drying time (considering microwave "on" times) (Table 4), and more uniform heat distribution within the product, resulting in better preservation of microstructure (Dehghannya et al., 2019).

Overall, the highest and lowest rehydration ratio values were noticed in the treatments with 900 W and a pulse ratio of 6, and 360 W with a pulse ratio of 1 (after the control treatment), respectively (Table 6). The rehydration ratio increased significantly by 28.96% with simultaneous increases in microwave power and pulse ratio. This enhancement can be attributed to the favorable influence of these conditions on reducing drying time (by considering microwave “on” times) (Table 4), preserving capillary structures and vascular integrity (less rupture), and minimizing shrinkage (Fig. 12) and bulk density (Fig. 13). On the other hand, the control treatment had the lowest rehydration ratio value among all treatments (Fig. 14), as the use of hot air alone could lead to more structural damage and vascular tissue destruction (more rupture) due to the extended drying time (Fig. 6), ultimately reducing water flow

Table 9
Shrinkage rate (m/s) of different treatments for corners and top and bottom surfaces of potato samples during drying for various microwave power (P; W) and pulse ratio (PR; dimensionless).

Treatment	P	PR	Corner	Top & bottom
1	0	0	$-5.851 \times 10^{-8} \pm 3.207 \times 10^{-10}$	$-1.092 \times 10^{-6} \pm 3.207 \times 10^{-8}$
2	360	1	$-1.824 \times 10^{-7} \pm 3.891 \times 10^{-9}$	$-2.046 \times 10^{-6} \pm 1.019 \times 10^{-7}$
3	360	2	$-1.492 \times 10^{-7} \pm 4.598 \times 10^{-9}$	$-1.698 \times 10^{-6} \pm 9.392 \times 10^{-8}$
4	360	4	$-1.138 \times 10^{-7} \pm 3.259 \times 10^{-9}$	$-1.375 \times 10^{-6} \pm 5.370 \times 10^{-8}$
5	360	6	$-8.604 \times 10^{-8} \pm 4.859 \times 10^{-9}$	$-1.104 \times 10^{-6} \pm 4.261 \times 10^{-8}$
6	600	1	$-1.869 \times 10^{-7} \pm 1.596 \times 10^{-9}$	$-2.023 \times 10^{-6} \pm 7.027 \times 10^{-8}$
7	600	2	$-1.473 \times 10^{-7} \pm 9.818 \times 10^{-9}$	$-1.700 \times 10^{-6} \pm 8.503 \times 10^{-8}$
8	600	4	$-1.184 \times 10^{-7} \pm 1.010 \times 10^{-8}$	$-1.416 \times 10^{-6} \pm 9.472 \times 10^{-8}$
9	600	6	$-1.008 \times 10^{-7} \pm 3.493 \times 10^{-9}$	$-1.196 \times 10^{-6} \pm 5.332 \times 10^{-8}$
10	900	1	$-1.676 \times 10^{-7} \pm 1.101 \times 10^{-8}$	$-1.199 \times 10^{-6} \pm 1.260 \times 10^{-7}$
11	900	2	$-1.509 \times 10^{-7} \pm 1.045 \times 10^{-8}$	$-1.660 \times 10^{-6} \pm 5.229 \times 10^{-8}$
12	900	4	$-1.240 \times 10^{-7} \pm 1.283 \times 10^{-8}$	$-1.490 \times 10^{-6} \pm 9.755 \times 10^{-8}$
13	900	6	$-1.003 \times 10^{-7} \pm 9.146 \times 10^{-9}$	$-1.346 \times 10^{-6} \pm 1.372 \times 10^{-7}$

within the dried product and thus lowering rehydration ratio (Dehghannya et al., 2018b).

3.7. Energy consumption

Fig. 15 illustrates the changes in energy consumption (microwave stage, hot air stage, and total energy consumed) at various powers and pulse ratios. Energy consumption was lower in the microwave stage compared to the hot air stage, due to the shorter drying time, more significant reduction in moisture content (Table 4), and higher drying rate (Fig. 10) during this stage. Energy consumption decreased by 3.4% with increasing microwave power (Table 7). This aligned with the Luka et al. (2023) and Macedo et al. (2024), and can be attributed to the increased drying rate at higher power levels, reducing drying time, enhancing D_{eff} (Table 7), and increasing mass transfer due to higher microwave energy and more heat generation (Dehghannya et al., 2021; Luka et al., 2023). Furthermore, energy consumption significantly decreased by 28.4% with increasing pulse ratio. A similar trend was observed in Song et al. (2024). This outcome can be attributed to the reduction in microwave "on" times at higher pulse ratios (Table 1), reduced drying time (considering microwave "on" times) (Table 4), and increased D_{eff} (Table 7) (Ali et al., 2023).

3.8. Appearance

Fig. 16 displays images of dried potato samples processed at various powers and pulse ratios. Visual assessment indicated that samples subjected to higher microwave power levels (600 and 900 W) and a pulse ratio of 6 exhibited superior structural integrity, characterized by minimized shrinkage (Fig. 12), reduced microstructural degradation, enhanced porosity (puffiness), and lower bulk density (Fig. 13). Generally, the dried sample at 360 W with a pulse ratio of 6 was more desirable due to reduced thermal energy from microwaves at lower powers, as well as shorter microwave on-times at higher pulse ratios (Table 1), leading to less degradation of pigments in terms of clarity and color.

3.9. Modeling and validation

Thirteen treatments were examined to assess the profiles of electromagnetic waves, moisture, and heat as per Table 8. The shrinkage rate at the edges and upper and lower surfaces of the product (Fig. 2) was considered according to Eq. (51) and Eq. (52) (applying the moving boundary) for various power and pulse ratio levels, including the control treatment (HA) (Table 9). Additionally, the initial moisture (5 g water/g dry solids) and the initial temperature (25 °C) at the start of the drying were supposed to be homogeneous. The maximum time required to hit the desired moisture (0.1 g water/g dry solids) for treatments 1 to 13 (Table 8) was set at 300, 95, 108, 130, 148, 89, 98, 108, 118, 86, 92, 99, and 105 min, respectively.

Fig. 17 illustrates the distribution of the electric field distribution across different powers and pulse ratios. The electric field (V/m) generates heat for drying potatoes using microwave radiation (Raj and Dash, 2021). Results showed that the electric field strength in the interior was more substantial due to the volumetric heating of microwave radiation compared to the edges. In other words, a higher electric field indicates that more heat is being applied to that part of the food, and if overheating occurs during the drying process, burning will initially start from that region (Bakshi et al., 2023; Raj and Dash, 2021). Furthermore, the results indicated that the electric field strength increased with higher microwave power due to increased energy generation (Raj and Dash, 2021). On the other hand, the electric field also increased with a higher pulse ratio due to reduced microwave “on” times (Table 1) and a more uniform distribution of waves in the product. The average electric field obtained in treatments 2 to 13 (Table 8) were 2930.0, 2955.1, 3006.3, 3042.0, 3756.3, 3787.4, 3813.2, 3822.9, 4594.2, 4606.2, 4641.1, and 4679.4 V/m, respectively.

Fig. 18 shows the temperature and moisture profiles after the drying stage with microwaves and after the drying stage with warm air (completion of drying), along with the control treatment (HA) at different power and pulse ratios. In the control treatment, the moisture and temperature profiles were shown after 150 (mid-drying) and 300 min (completion of drying). According to the temperature profiles in Fig. 18, temperature increased with higher microwave power, which can be attributed to increased thermal energy at higher power levels. Moreover, temperature increased with a higher pulse ratio, which can be explained by the increased electric field at higher pulse ratios (Fig. 17). The average temperatures achieved in treatments 1 to 13 (Table 8) were 39.5, 36.3, 38.0, 40.5, 42.0, 36.0, 39.5, 42.3, 43.5, 37.0, 40.5, 43.6, and 46.0 °C, respectively. A comparison of the temperature profiles during convective warm air drying (control treatment) and combined microwave and warm air drying showed that in the control treatment, due to the heating mechanism from the surface to the interior of the product, the surface temperature was higher than the internal temperature. In contrast, in the combined method, due to the volumetric heating mechanism of microwave radiation from the inside to the surface of the potato, the internal temperature was higher than the surface temperature. Additionally, a comparison of the profiles of dried potatoes in the middle and at the end of the drying process (Fig. 18) indicated the impact of considering shrinkage (moving boundary; MB); samples dried at the end of drying were significantly smaller than those dried in the middle of the process. Furthermore, the profiles of dried potatoes at

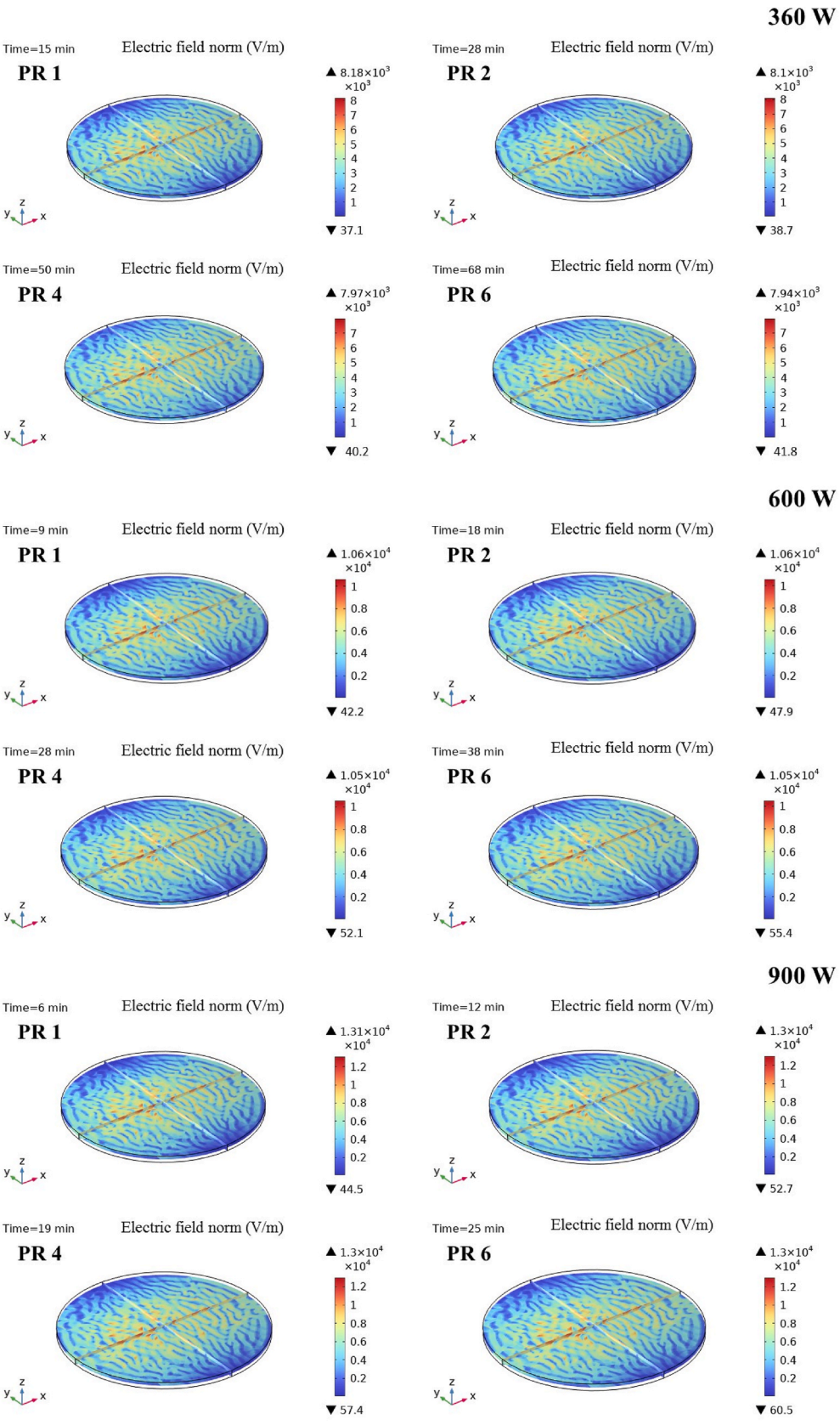

Fig. 17. Electric field distribution at different microwave powers (360, 600 and 900 W) and pulse ratios (1, 2, 4 and 6).

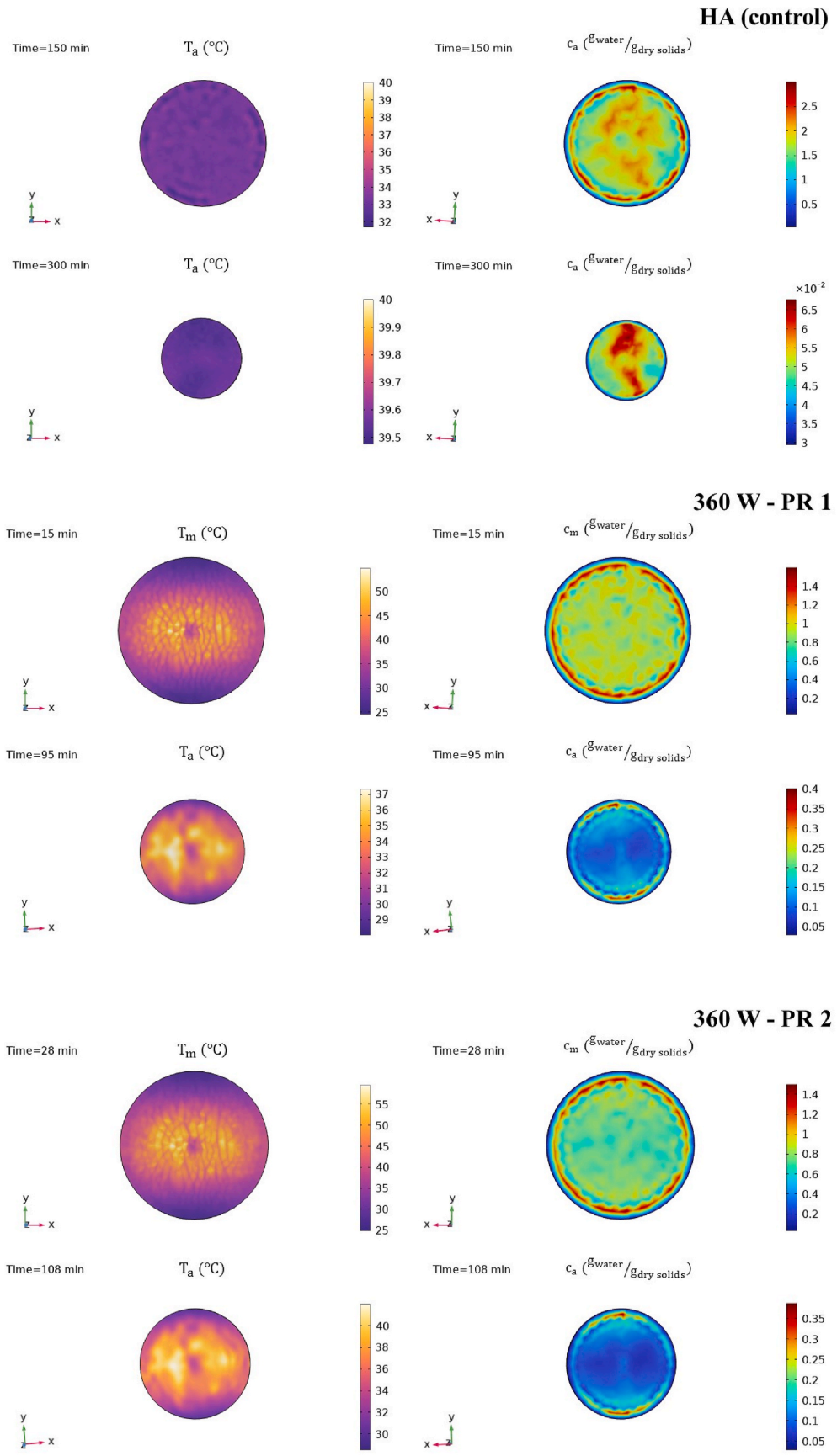

Fig. 18. Profiles of temperature (T) and moisture (c) after the completion of the drying stage with microwave (T_m and c_m) and the completion of the drying stage with hot air (T_a and c_a) at microwave powers of 0 (HA), 360, 600 and 900 W and pulse ratios of 1, 2, 4 and 6.

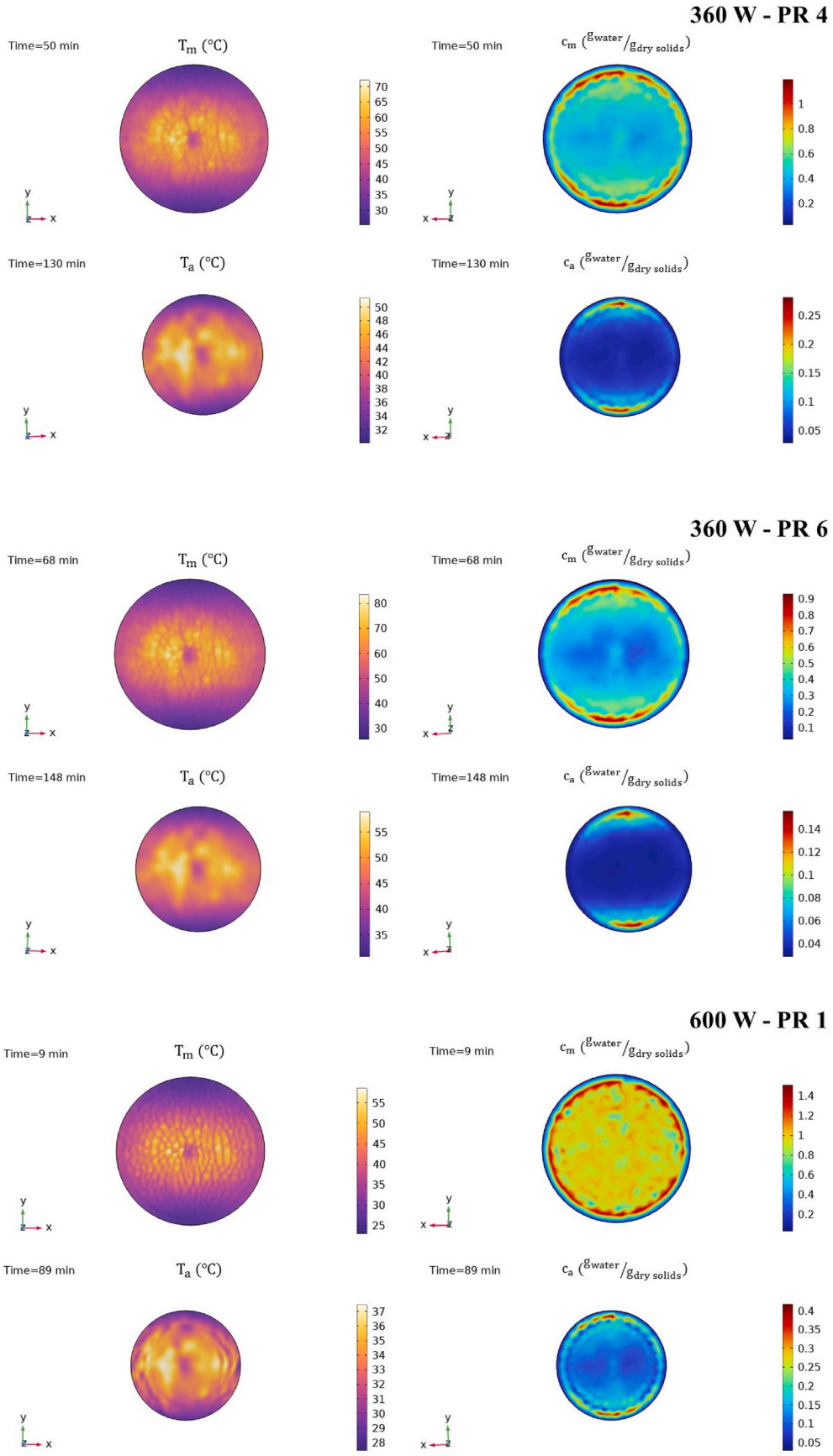

Fig. 18. (*continued*).

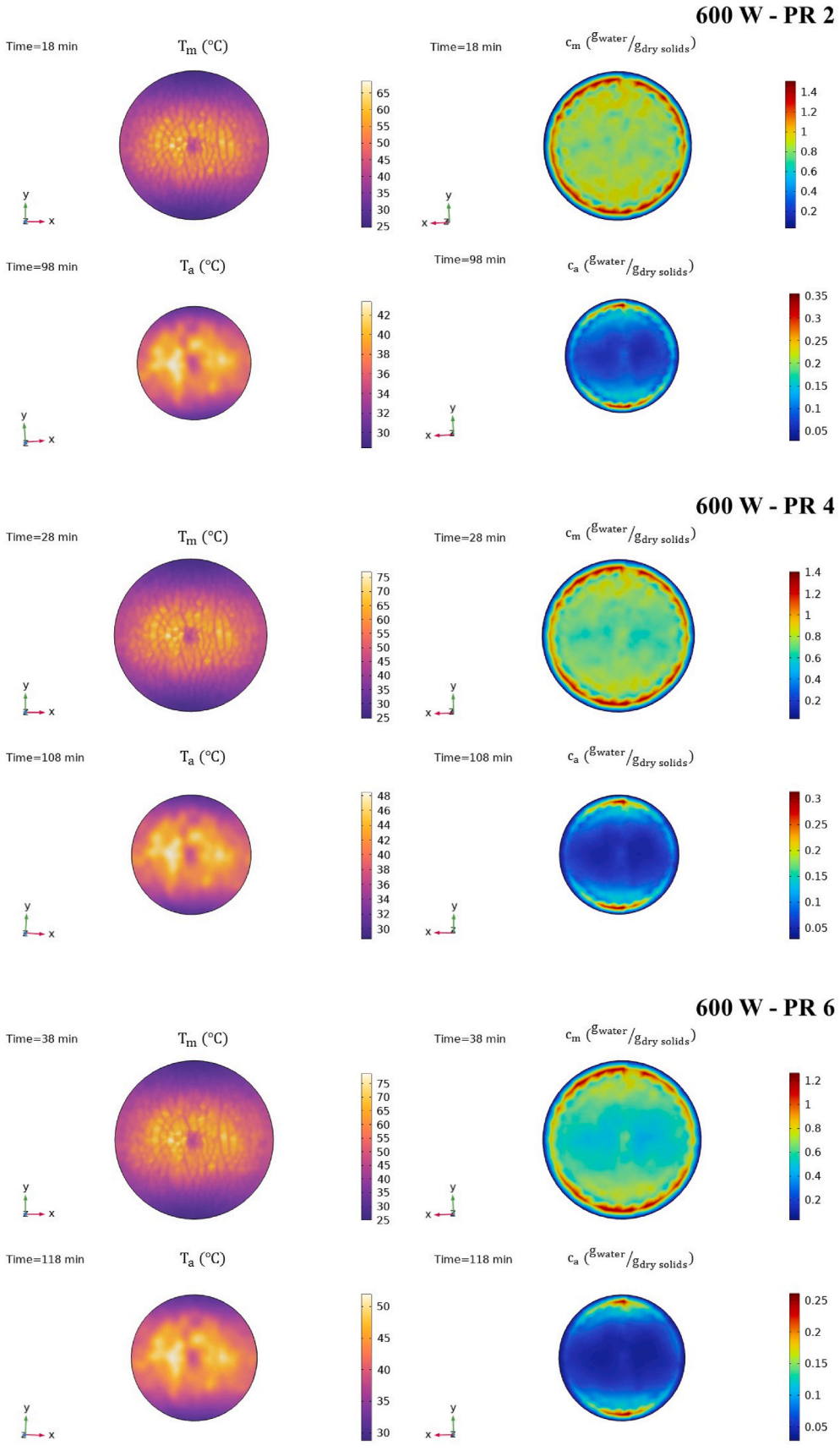

Fig. 18. (*continued*).

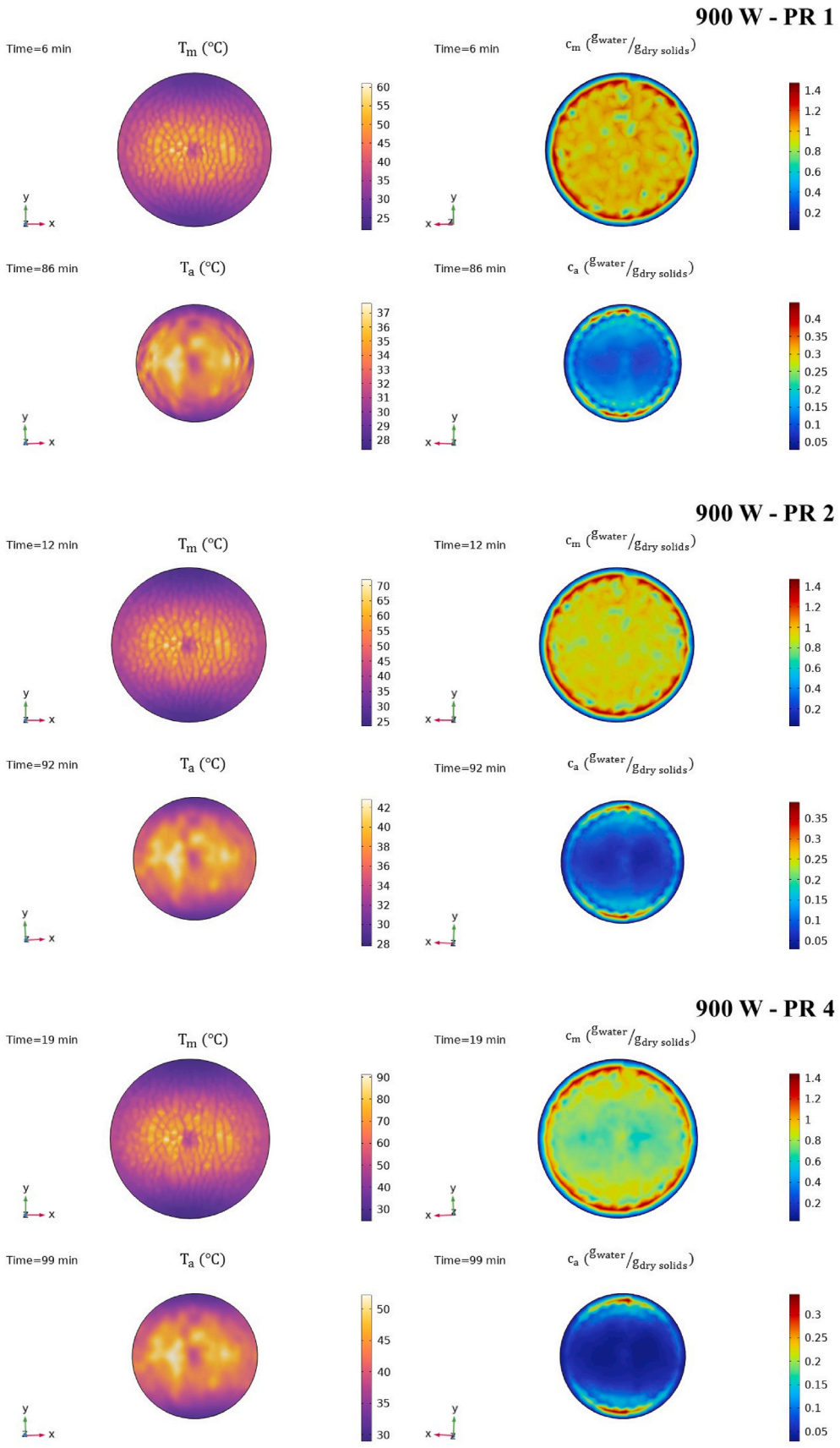

Fig. 18. (*continued*).

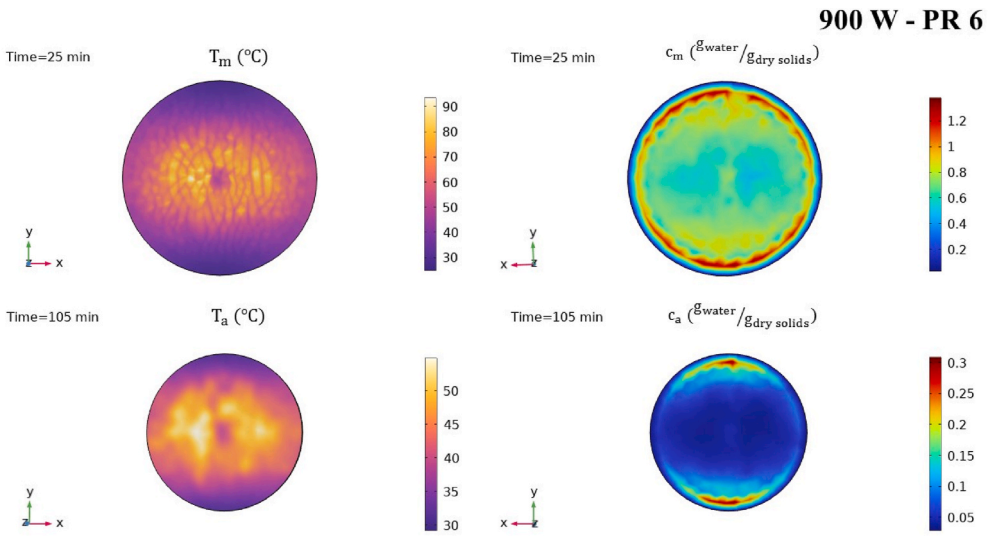

Fig. 18. (*continued*).

higher power and pulse ratios exhibited less shrinkage (volume reduction), with the highest shrinkage observed in the samples dried using warm air alone (HA). This can be attributed to the longer drying time using only warm air (300 min) compared to other treatments, and also to the reduced drying time (regarding the microwave "on" times) at higher power and pulse ratios (Table 4). These findings align with experimental shrinkage measurements (Fig. 12).

On the other hand, according to the moisture profiles in Fig. 18, moisture content decreased with higher microwave power, which was associated with enhanced volumetric heating at higher power levels and, accordingly, more moisture removal. Additionally, moisture content also decreased with higher microwave pulse ratios, which can be explained by increased temperature, extended total drying time (Table 4), and, subsequently, more moisture removal. A comparison of the moisture profiles in convective warm air drying (control treatment) and combined microwave and warm air drying showed that in the combined method, due to the unique volumetric heating mechanism of microwaves and the heat transfer direction from inside to the surface of the potato, the moisture inside the food was lower than at the surface. In contrast, in the control treatment, due to the heating mechanism from the surface to the inside of the product, surface moisture was lower than internal moisture. In other words, moisture was first removed from the surface and then from inside the potato. In summary, moisture removal in convective warm air drying (control treatment) occurred starting from the edges of the food, unlike the combined method of microwave and warm air drying.

Fig. 19 illustrates the moisture content of potatoes regarding experimental and simulated data for different powers and pulse ratios. Additionally, Table 10 presents the final experimental and simulated moisture content. According to Table 10, potato samples dried at 900 W and pulse ratio 6 exhibited lower final moisture content than other treatments. Higher heat transfer at higher powers allowed for quicker heating, considering the higher inner water vapor pressure and, subsequently, a more substantial reduction in moisture content (Table 4) and an increased drying rate (Table 5) (Aghilinategh et al., 2015). Furthermore, at higher pulse ratios, due to less structural damage owing to lower "on" times (Table 1), moisture removal was facilitated within the product (Luka et al., 2023).

Fig. 20 shows the general model execution regarding the comparison of experimental and simulated moisture content across all treatments derived from all power and pulse ratio levels. According to this figure, the results obtained from validation, represented by R^2 and RMSE (0.989 and 0.1968, respectively), indicate a good agreement between the experimental and simulation data, which describes the efficiency of this modeling during the drying process.

4. Conclusion

The interactive effects of power and pulse ratio of microwaves were evaluated to simultaneously examine these variables along with the control treatment (HA) on the combined drying process of potatoes. Moisture removal and effective diffusivity (D_{eff}) increased with higher power and pulse ratios (reduced "on" times of microwaves) due to more significant volumetric heating and increased internal vapor pressure. Additionally, higher power and pulse ratios led to reduced shrinkage and, consequently, reduced bulk density; this was attributed to the more homogeneous distribution of heat and moisture within the product owing to lower microwaves "on" times and hence, shorter drying time when considering microwave "on" times. The rehydration ratio rate also increased with higher power and pulse ratio, which was associated with reduced drying time (regarding microwave "on" times) and, consequently, better preservation of vascular tissues and improved water transfer within the product. In general, the final moisture content, shrinkage, and bulk density decreased by 15.55%, 26.28%, and 13.22%, respectively, with increasing power and pulse ratio. In contrast, D_{eff} and rehydration ratio increased by 14.28% and 28.96%, respectively, with increasing power and pulse ratio. The energy consumption rate decreased with higher power and pulse ratios due to increased mass transfer. Furthermore, a simulation of the process to examine the effect of power and microwave pulse ratio considering the moving boundary to account for the effect of shrinkage was performed, and model validation using R^2 and RMSE (0.989 and 0.1968) indicated good agreement between the experimental and predicted data. Overall, this investigation demonstrated that the combined intermittent microwave and warm air drying with fixed off-times and varying "on" times can be utilized in the food industry to optimize quality and efficiency.

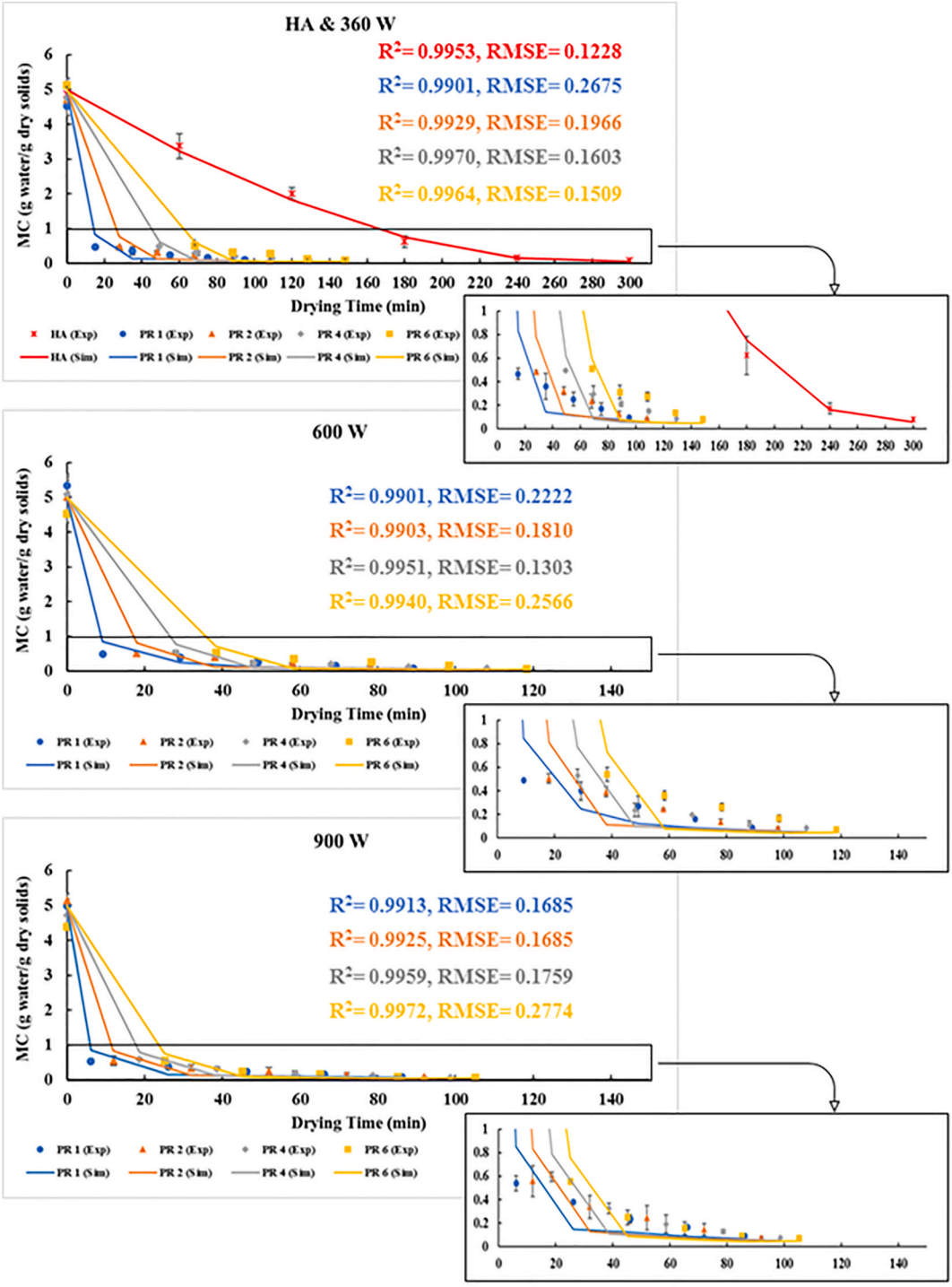

Fig. 19. Moisture content variations of potato samples at different microwave powers of 0 (HA), 360, 600 and 900 W and pulse ratios of 1, 2, 4 and 6: Comparison of experimental (Exp) and simulation (Sim) data.

Table 10
Final moisture content (MC) for experimental and simulation data ($g_{water}/g_{dry\ solids}$).

Treatment	Microwave power (W)	Microwave pulse ratio	Experimental MC	Predicted MC
1	0	0	0.083 ± 0.004	0.061
2	360	1	0.096 ± 0.002	0.073
3	360	2	0.092 ± 0.001	0.059
4	360	4	0.088 ± 0.003	0.054
5	360	6	0.082 ± 0.005	0.048
6	600	1	0.088 ± 0.009	0.069
7	600	2	0.084 ± 0.008	0.062
8	600	4	0.085 ± 0.007	0.053
9	600	6	0.074 ± 0.008	0.049
10	900	1	0.090 ± 0.008	0.070
11	900	2	0.078 ± 0.007	0.059
12	900	4	0.075 ± 0.004	0.055
13	900	6	0.073 ± 0.016	0.051

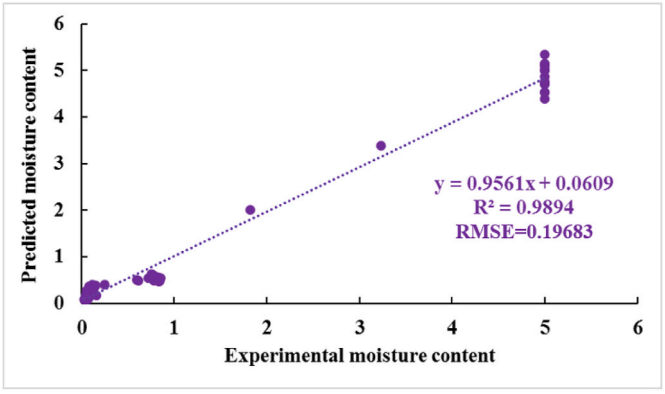

Fig. 20. The overall model performance comparing the experimental and predicted data in all treatments resulting from the microwave powers of 0 (HA), 360, 600 and 900 W and pulse ratios of 1, 2, 4 and 6.

Nomenclature

c	Concentration ($g_{water}/g_{dry\ solids}$)
Cp	Specific heat capacity (J/kg.K)
D	Diameter (cm)
D_{eff}	Effective moisture diffusion coefficient (m^2/s)
DR	Drying rate ($g_{water}/g_{dry\ solids}$.min)
Exp	Experimental
f	Frequency (Hz)
h	Convective heat transfer coefficient ($W/m^2.K$)
HA	Hot air
k	Thermal conductivity coefficient (W/m.K)
k_c	Convective mass transfer coefficient (m/s)
L	Thickness (cm)
MB	With moving boundary
MC	Moisture content ($g_{water}/g_{dry\ solids}$)
MR	Moisture ratio (Dimensionless)
MW	Microwave
NO-MB	Without moving boundary
Nu	Nusselt number (Dimensionless)
P	Power (W)
Pr	Prandtl number (Dimensionless)
PR	Pulse ratio (Dimensionless)
R^2	Coefficient of determination
Re	Reynolds number (Dimensionless)
RMSE	Root mean square error
RR	Rehydration ratio (Dimensionless)
Sim	Simulation
T	Temperature (°C)
t	Time (s)
V	Velocity (m/s)
Greek symbols	
α	Thermal diffusion coefficient (m^2/s)
λ	Latent heat of evaporation (J/kg)
ε'	Dielectric constant (Dimensionless)
ε''	Dielectric loss factor (Dimensionless)
μ	Dynamic viscosity (Pa.s)
ρ	Density (kg/m^3)
Subscripts	
0	Reference
a	Hot air stage
e	Equilibrium
ev	Evaporation
ext	Surrounding air in the oven
m	Microwave stage
P	Potato
s	Solid
w	Water

(*continued on next column*)

(*continued*)

CRediT authorship contribution statement

Jalal Dehghannya: Conceptualization, Funding acquisition, Investigation, Methodology, Project administration, Resources, Software, Supervision, Validation, Visualization, Writing – review & editing. **Mahdi Habibi-Ghods:** Data curation, Formal analysis, Investigation, Methodology, Software, Visualization, Writing – original draft.

Declaration of competing interest

The authors declare that they have no known competing financial interests or personal relationships that could have appeared to influence the work reported in this paper.

Data availability

All data generated or analyzed during this study are included in this manuscript.

References

Aghilinategh, N., Rafiee, S., Gholikhani, A., Hosseinpur, S., Omid, M., Mohtasebi, S.S., Maleki, N., 2015. A comparative study of dried apple using hot air, intermittent and continuous microwave: evaluation of kinetic parameters and physicochemical quality attributes. Food Sci. Nutr. 3, 519–526.

Ali, A., Chua, B.L., Chow, Y.H., Tee, L.H., 2023. Quality and energy efficiency evaluation of *Rosmarinus officinalis* L. by intermittent and continuous microwave drying: polyphenol composition, bioactive compounds quantification, antioxidant properties, physical characteristics, and energy consumption. J. Food Process. Eng. 46, e14453.

Aprajeeta, J., Gopirajah, R., Anandharamakrishnan, C., 2015. Shrinkage and porosity effects on heat and mass transfer during potato drying. J. Food Eng. 144, 119–128.

Bakshi, N., Jain, S., Raman, A., Pant, T., 2023. Microwave: an overview. In: Nayik, G.A., Ranjha, M., Zeng, X.A., Irfan, S., Zahra, S.M. (Eds.), Ultrasound and Microwave for Food Processing. Academic Press, Cambridge, USA, pp. 19–59.

Brahmi, F., Mateos-Aparicio, I., Mouhoubi, K., Guemouni, S., Sahki, T., Dahmoune, F., Belmehdi, F., Bessai, C., Madani, K., Boulekbache-Makhlouf, L., 2023. Kinetic modeling of convective and microwave drying of potato peels and their effects on antioxidant content and capacity. Antioxidants 12, 638.

Chatzilia, T., Kaderides, K., Goula, A.M., 2023. Drying of peaches by a combination of convective and microwave methods. J. Food Process. Eng. 46, e14296.

Chayjan, R.A., Kaveh, M., Khayati, S., 2015. Modeling drying characteristics of hawthorn fruit under microwave-convective conditions. J. Food Process. Preserv. 39, 239–253.

Chen, Y., Song, C., Li, Z., Chen, H., Jin, G., 2020. Effects of hot air and combined microwave and hot air drying on the quality attributes of celery stalk slices. J. Food Process. Preserv. 44, e14310.

Chong, C.H., Figiel, A., Szummy, A., Wojdyło, A., Chua, B.L., Khek, C.H., Yuan, M.C., 2021. Herbs drying. In: Galanakis, C.M. (Ed.), Aromatic Herbs in Food. Academic Press, Cambridge, USA.

Dai, J.-W., Xiao, H.-W., Zhang, L.-H., Chu, M.-Y., Qin, W., Wu, Z.-J., Han, D.-D., Li, Y.-L., Liu, Y.-W., Yin, P.-F., 2019. Drying characteristics and modeling of apple slices during microwave intermittent drying. J. Food Process. Eng. 42, e13212.

Dehghannya, J., Farshad, P., Khakbaz Heshmati, M., 2018a. Three-stage hybrid osmotic–intermittent microwave–convective drying of apple at low temperature and short time. Dry. Technol. 36, 1982–2005.

Dehghannya, J., Hosseinlar, S.-H., Heshmati, M.K., 2018b. Multi-stage continuous and intermittent microwave drying of quince fruit coupled with osmotic dehydration and low temperature hot air drying. Innov. Food Sci. Emerg. Technol. 45, 132–151.

Dehghannya, J., Pourahmad, M., Ghanbarzadeh, B., Ghaffari, H., 2018c. Heat and mass transfer modeling during foam-mat drying of lime juice as affected by different ovalbumin concentrations. J. Food Eng. 238, 164–177.
Dehghannya, J., Kadkhodaei, S., Heshmati, M.K., Ghanbarzadeh, B., 2019. Ultrasound-assisted intensification of a hybrid intermittent microwave - hot air drying process of potato: quality aspects and energy consumption. Ultrasonics 96, 104–122.
Dehghannya, J., Aghazade-Khoie, E., Khakbaz Heshmati, M., Ghanbarzadeh, B., 2020. Influence of ultrasound intensification on the continuous and pulsed microwave during convective drying of apple. Int. J. Fruit Sci. 20, S1751–S1764.
Dehghannya, J., Seyed-Tabatabaei, S.-R., Khakbaz Heshmati, M., Ghanbarzadeh, B., 2021. Influence of three stage ultrasound—intermittent microwave—hot air drying of carrot on physical properties and energy consumption. Heat Mass Tran. 57, 1893–1907.
Dehghannya, J., Farhoudi, S., Dadashi, S., 2023a. Investigation of microwave application time with constant pulse ratio on drying of zucchini. Food Sci. Nutr. 11, 4794–4811.
Dehghannya, J., Rastgou-Oskuei, S., Dadashi, S., 2023b. Influence of pulsed microwave on betacyanins, betaxanthins and physical properties during drying of red beetroot. Appl.Food Res. 3, 100305.
Devaux, A., Goffart, J.-P., Kromann, P., Andrade-Piedra, J., Polar, V., Hareau, G., 2021. The potato of the future: opportunities and challenges in sustainable agri-food systems. Potato Res. 64, 681–720.
Emam-Djomeh, Z., Dehghannya, J., Sotudeh Gharabagh, R., 2006. Assessment of osmotic process in combination with coating on effective diffusivities during drying of apple slices. Dry. Technol. 24, 1159–1164.
Erle, U., Pesheck, P., Lorence, M., 2020. Development of Packaging and Products for Use in Microwave Ovens, second ed. Woodhead Publishing, Sawston, UK.
Franco, A.P., Yamamoto, L.Y., Tadini, C.C., Gut, J.A.W., 2015. Dielectric properties of green coconut water relevant to microwave processing: effect of temperature and field frequency. J. Food Eng. 155, 69–78.
Fricke, B.A., Becker, B.R., 2001. Evaluation of thermophysical property models for foods. HVAC R Res. 7, 311–330.
Gomide, A.I., Monteiro, R.L., Laurindo, J.B., 2022. Impact of the power density on the physical properties, starch structure, and acceptability of oil-free potato chips dehydrated by microwave vacuum drying. LWT - Food Sci. Technol. (Lebensmittel-Wissenschaft -Technol.) 155, 112917.
Heshmati, M.K., Khiavi, H.D., Dehghannya, J., Baghban, H., 2023. 3D simulation of momentum, heat and mass transfer in potato cubes during intermittent microwave-convective hot air drying. Heat Mass Tran. 59, 239–254.
Huang, D., Men, K., Tang, X., Li, W., Sherif, S., 2021. Microwave intermittent drying characteristics of *camellia oleifera* seeds. J. Food Process. Eng. 44, e13608.
Kumar, C., Karim, M.A., 2019. Microwave-convective drying of food materials: a critical review. Crit. Rev. Food Sci. Nutr. 59, 379–394.
Kumar, C., Joardder, M.U.H., Farrell, T.W., Millar, G.J., Karim, M.A., 2016. Mathematical model for intermittent microwave convective drying of food materials. Dry. Technol. 34, 962–973.
Kumar, C., Joardder, M.U.H., Farrell, T.W., Karim, M.A., 2018. Investigation of intermittent microwave convective drying (IMCD) of food materials by a coupled 3D electromagnetics and multiphase model. Dry. Technol. 36, 736–750.
Luka, B.S., Vihikwagh, Q.M., Ngabea, S.A., Mactony, M.J., Zakka, R., Yuguda, T.K., Adnouni, M., 2023. Convective and microwave drying kinetics of white cabbage (*Brassica oleracae* var *capitata* L.): mathematical modelling, thermodynamic properties, energy consumption and reconstitution kinetics. J. Agric. Food Res. 12, 100605.
Macedo, L.L., Corrêa, J.L.G., Petri Júnior, I., Araújo, C.d.S., Vimercati, W.C., 2022. Intermittent microwave drying and heated air drying of fresh and isomaltulose (Palatinose) impregnated strawberry. LWT - Food Sci. Technol. (Lebensmittel-Wissenschaft -Technol.) 155, 112918.
Macedo, L.L., Corrêa, J.L.G., Júnior, I.P., Vimercati, W.C., Araújo, C.D.S., 2024. Intermittent microwave drying of strawberry fruits. In: Advanced Research Methods in Food Processing Technologies. Apple Academic Press, Florida, USA, pp. 257–268.
Malafronte, L., Lamberti, G., Barba, A.A., Raaholt, B., Holtz, E., Ahrné, L., 2012. Combined convective and microwave assisted drying: experiments and modeling. J. Food Eng. 112, 304–312.
Mierzwa, D., Szadzińska, J., 2019. The microwave-assisted convective drying of kale (*Brassica oleracea* L. var. *sabellica* L.) using continuous and changeable power radiation. J. Food Process. Eng. 42, e13004.
Monteiro, R.L., de Moraes, J.O., Domingos, J.D., Carciofi, B.A.M., Laurindo, J.B., 2020. Evolution of the physicochemical properties of oil-free sweet potato chips during microwave vacuum drying. Innov. Food Sci. Emerg. Technol. 63, 102317.
Nguyen, T.-V.-L., Nguyen, P.-B.-D., Luu, X.-C., Huynh, B.-L., Krishnan, S., Huynh, P.T., 2019. Kinetics of nutrient change and color retention during low-temperature microwave-assisted drying of bitter melon (*Momordica charantia* L.). J. Food Process. Preserv. 43, e14279.
Onyenwigwe, D.I., Ndukwu, M.C., Igbojionu, D.O., Ugwu, E.C., Nwakuba, N.R., Mbanaso, J., 2023. Mathematical modelling of drying kinetics, economic and environmental analysis of natural convection mix-mode solar and sun drying of pre-treated potato slices. Int. J. Ambient Energy 44, 1721–1732.
Pavón-Melendez, G., Hernández, J.A., Salgado, M.A., Garcı, x. M.A. a, 2002. Dimensionless analysis of the simultaneous heat and mass transfer in food drying. J. Food Eng. 51, 347–353.
Perussello, C.A., Kumar, C., de Castilhos, F., Karim, M.A., 2014. Heat and mass transfer modeling of the osmo-convective drying of yacon roots (*Smallanthus sonchifolius*). Appl. Therm. Eng. 63, 23–32.
Pham, N.D., Martens, W., Karim, M.A., Joardder, M.U.H., 2018. Nutritional quality of heat-sensitive food materials in intermittent microwave convective drying. Food Nutr. Res. 62, 1292.
Raj, G.V.S.B., Dash, K.K., 2021. Heat transfer analysis of convective and microwave drying of dragon fruit. J. Food Process. Eng. 44, e13775.
Rao, R.S., 2015. Microwave Engineering, second ed. PHI Learning Pvt. Ltd., Delhi, India.
Rodríguez-Ramírez, J., Méndez-Lagunas, L., López-Ortiz, A., Torres, S.S., 2012. True density and apparent density during the drying process for vegetables and fruits: a review. J. Food Sci. 77, R146–R154.
Song, F., Zhang, N., Liu, P., Liu, Z., Fu, W., Li, Z., Song, C., 2024. Heating uniformity improvement of the intermittent microwave drying for carrot with simulations and experiments. J. Food Process. Eng. 47, e14581.
von Horstig, M.-W., Schoo, A., Loellhoeffel, T., Mayer, J.K., Kwade, A., 2022. A perspective on innovative drying methods for energy-efficient solvent-based production of lithium-ion battery electrodes. Energy Technol. 10, 2200689.